

RESEARCH

Open Access



Neuropeptide Y in the medial habenula alleviates migraine-like behaviors through the Y1 receptor

Chunxiao Yang^{1,2}, Zihua Gong^{2,3,4}, Xiaochen Zhang⁵, Shuai Miao^{2,3}, Bozhi Li², Wei Xie^{2,3}, Tao Wang^{2,3}, Xun Han², Liang Wang⁶, Zhao Dong^{1,2,3} and Shengyuan Yu^{1,2,3*} 

Abstract

Background Migraine is a highly disabling health burden with multiple symptoms; however, it remains undertreated because of an inadequate understanding of its neural mechanisms. Neuropeptide Y (NPY) has been demonstrated to be involved in the modulation of pain and emotion, and may play a role in migraine pathophysiology. Changes in NPY levels have been found in patients with migraine, but whether and how these changes contribute to migraine is unknown. Therefore, the purpose of this study was to investigate the role of NPY in migraine-like phenotypes.

Methods Here, we used intraperitoneal injection of glyceryl trinitrate (GTN, 10 mg/kg) as a migraine mouse model, which was verified by light-aversive test, von Frey test, and elevated plus maze test. We then performed whole-brain imaging with NPY-GFP mice to explore the critical regions where NPY was changed by GTN treatment. Next, we microinjected NPY into the medial habenula (MHb), and further infused Y1 or Y2 receptor agonists into the MHb, respectively, to detect the effects of NPY in GTN-induced migraine-like behaviors.

Results GTN effectively triggered allodynia, photophobia, and anxiety-like behaviors in mice. After that, we found a decreased level of GFP⁺ cells in the MHb of GTN-treated mice. Microinjection of NPY attenuated GTN-induced allodynia and anxiety without affecting photophobia. Furthermore, we found that activation of Y1—but not Y2—receptors attenuated GTN-induced allodynia and anxiety.

Conclusions Taken together, our data support that the NPY signaling in the MHb produces analgesic and anxiolytic effects through the Y1 receptor. These findings may provide new insights into novel therapeutic targets for the treatment of migraine.

Keywords Migraine, Glyceryl trinitrate, Neuropeptide Y, Y1 receptor, Medial habenula

*Correspondence:

Shengyuan Yu

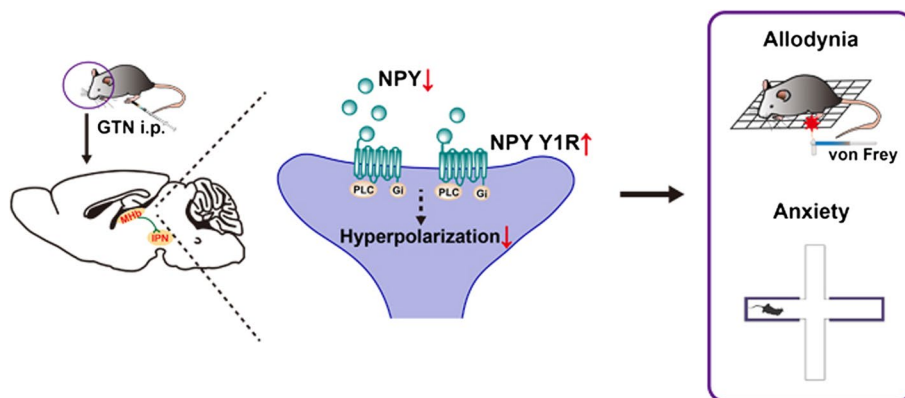
yusy1963@126.com; yushengyuan@301hospital.com.cn

Full list of author information is available at the end of the article



© The Author(s) 2023. **Open Access** This article is licensed under a Creative Commons Attribution 4.0 International License, which permits use, sharing, adaptation, distribution and reproduction in any medium or format, as long as you give appropriate credit to the original author(s) and the source, provide a link to the Creative Commons licence, and indicate if changes were made. The images or other third party material in this article are included in the article's Creative Commons licence, unless indicated otherwise in a credit line to the material. If material is not included in the article's Creative Commons licence and your intended use is not permitted by statutory regulation or exceeds the permitted use, you will need to obtain permission directly from the copyright holder. To view a copy of this licence, visit <http://creativecommons.org/licenses/by/4.0/>. The Creative Commons Public Domain Dedication waiver (<http://creativecommons.org/publicdomain/zero/1.0/>) applies to the data made available in this article, unless otherwise stated in a credit line to the data.

Graphical Abstract



Introduction

Migraine is a complex, widespread, and paroxysmal neurologic disorder, affecting ~15% of the global population [1]. During the COVID-19 pandemic, a worsening of migraines was found in more than half of migraineurs [2]. Migraine is punctuated by a broad spectrum of sensory dysfunctions apart from headaches—including photophobia, phonophobia, osmophobia, and cutaneous allodynia [3]. In addition to pan-sensory gain, nausea and vomiting are prominent features, and patients can be physically, mentally, and socially incapacitated for days by migraine attacks [4]. Moreover, migraine is often associated with comorbid diseases, including epilepsy [5], depression and anxiety [6, 7], stroke [8], and other conditions [9]. These characteristics have led migraine to emerge as the second leading cause of disability [10]. Although there are various acute and prophylactic therapies for migraine, most focus only on headache-related symptoms while failing to address multisensory integration. Besides, currently available treatments are not effective in all patients with migraine [11]. Therefore, there is a clear and unmet need for additional refining of migraine management. Recently, neuropeptides and their receptors have gained much attention as novel treatments because of their proposed role in migraine pathogenesis [12]. Among them, neuropeptide Y (NPY) is a strong potential candidate.

The 36-amino acid peptide, NPY, is widely distributed throughout the central and peripheral nervous systems and many other tissues. Of these, the brain is the most abundant site of NPY expression [13]. NPY has been considered to play an important role in numerous physiological processes, including food intake [14], pain processing [15], emotion regulating [16] and modulation of

cortical excitability [17]. All of these processes are known to be involved in migraine, suggesting a key role of NPY in migraine pathophysiology. The association between NPY levels and migraine has been extensively studied; however, no conclusions were reached. For example, Gallai et al. [18] reported that plasma NPY levels were decreased during the interictal period in juveniles with migraine, but increased during migraine attacks only in patients who experienced migraine with aura. In contrast, Siva et al. [19] showed higher serum NPY level in migraineurs during an attack-free period, and Goadsby et al. [20] showed that NPY levels in the external jugular venous blood remained unchanged during migraine attacks. Similar conflicting results were also found in cerebrospinal fluid [21, 22]. Considering the widespread expression of NPY in the brain, a deeper understanding of its variations in brain areas and its specific role in migraine is urgently needed.

NPY signals through four Y receptors in humans (Y1, Y2, Y4, and Y5) and Y6 in mice, all of which are expressed in the brain [23]. Naveilhan and colleagues [24] found that Y1-receptor-knockout mice displayed hyperalgesia and abolished the antinociceptive effects of NPY delivered intrathecally. Another study found that peripheral administration of NPY promoted pain via the Y2 receptor [25], suggesting a biphasic role of NPY in nociception at different sites with different receptors. Unfortunately, potential relationships between NPY levels and migraine remain uncertain. In addition, the Y5 receptor has been implicated in food intake [26] and hunger-dependent odor preferences [27]. While the Y4-receptor mRNA is the least-common NPY receptor subtype, it exhibits a much higher affinity for the pancreatic polypeptide than for NPY [28]. These data lead us to question the possible

role of NPY in migraine and which type of receptors are involved.

It is well accepted that systemic administration of glyceryl trinitrate (GTN, a nitric oxide donor) produces migraine-like symptoms in animals, similar to effects observed in humans, and sensitizes structures that underlie migraine pathophysiology [29, 30]. Thus, we used GTN to model migraine in mice and investigated the role of NPY in migraine-like phenotypes. Using a brain-wide mapping of NPY expression with NPY-GFP mice, we identified that NPY levels in the medial habenula (MHb) were significantly decreased in GTN mice. Furthermore, site-directed infusion of NPY and a Y1 receptor agonist alleviated GTN-induced allodynia and anxiety-like behaviors. Our data provide the first evidence that NPY signaling through the Y1 receptor in the MHb critically modulates migraine-like behaviors.

Methods

Animals

Male mice were used throughout the study to eliminate possible hormone cycle effects. SPF-grade wild-type (C57BL/6 J) mice (8–10 weeks old) purchased from SiPeiFu Biotechnology Co., Ltd (Beijing, China) were used for the phenotype experiments and immunofluorescence staining. NPY-GFP transgenic mice (JAX stock #006417) in which GFP is expressed from the *Npy* promoter [31] were used for VISoR imaging.

The mice were group housed under tightly controlled temperature (21°C–24°C), humidity (40%–60%), and illumination conditions (12-h light/dark cycle, lights on at 9:00 AM) and with ad libitum access to food and water. All experimental procedures were approved by the Institutional Animal Care and Use Committee of the Chinese People's Liberation Army (PLA) General Hospital, and animal experiments were conducted following the Animal Research: Reporting of in Vivo Experiments (ARRIVE) guidelines [32].

Glyceryl trinitrate (GTN) mouse model of migraine

Glyceryl trinitrate (GTN) is the most common and well-established experimental migraine trigger in humans and rodents [33]. GTN induces migraine-like attacks with allodynia and conditioned place aversion [34]. We administered GTN to investigate potential mechanisms associated with migraine headaches. Mice were randomly assigned to either a GTN or vehicle (VEH) group. Experimenters were blind to group allocation. GTN (5 mg/ml in ethanol, Beijing Yimin Pharmaceutical Co., Ltd., Beijing, China) was freshly diluted in 0.9% (wt/vol) saline to a final concentration of 0.5 mg/ml for a dose of 10 mg/kg [35]. The vehicle containing 10% (vol/vol) alcohol was

administered intraperitoneally in a 0.2 ml/10 g volume as a control. After administration, the mice were allowed to recover for at least 30 min in their home cages.

Cannula implantation and drug microinjection

For stereotaxic surgery, the mice were deeply anesthetized by intraperitoneal injection (0.2 ml/10 g body weight) of 1.25% Avertin (a mixture of 12.5 mg/mL of 2,2,2-Tribromoethanol and 25 μ l/mL 2-Methyl-2-butanol, Sigma, T48402, 152463, St. Louis, MO, USA), and then placed into a stereotaxic device (RWD Life Science, 69105, Shenzhen, China). After exposing the skull by scalp incision, bilateral craniotomies were created using a dental drill with 0.5-mm burs. Next, guide cannulas (27 gauge, 3.5 mm pedestal, RWD Life Science, 62004, Shenzhen, China) were implanted into the bilateral MHb (20° angle at the coordinates anteroposterior [AP] – 1.34 mm, mediolateral [ML] \pm 1.21 mm, and dorsoventral [DV] – 2.70 mm), according to the Paxinos & Franklin Mouse Brain Atlas [36]. The cannulas were secured to the skull with screws and dental cement, and the stylets were inserted to avoid obstruction of the cannulas. The mice were allowed to recover from surgery for 10 days before behavioral testing.

During drug infusion, mice were maintained under light isoflurane (1%–1.5%) anesthesia, the stylets were removed and injection cannulas (33 gauge, RWD Life Science, 62204, Shenzhen, China) were inserted 0.5 mm beyond the guide cannulas for a final distance of 2.75 mm from the brain's surface. The injection cannula was connected to a 10 μ l microsyringe (Hamilton, Nevada, USA) via a polyethylene tube driven by a syringe pump (KD Scientific, 788130, USA). NPY (2 μ g/ μ l in saline, Tocris Bioscience, 1153, UK), Y1R agonist ([Leu31,Pro34]-NPY, 2 μ g/ μ l in saline, MedChemExpress, HY-P1323A, Monmouth Junction, USA), Y2R agonist (Peptide YY, 2 μ g/ μ l in saline, MedChemExpress, HY-P1021A, Monmouth Junction, USA) or saline were infused bilaterally into the MHb at a flow rate of 100 nl/min (200 nl/side). The intracranial injection concentrations were determined based on previous studies [37, 38]. After injection, the cannulas were left in place for 5 min to allow for drug diffusion. Subsequently, the injection cannulas were removed and the stylets were re-inserted. Drug injections were performed immediately before induction of the GTN migraine mouse model. Cannula placements were verified postmortem by infusing 200 nl of 0.25% Evans Blue (Sigma, E2129, St. Louis, MO, USA) into the MHb before sacrifice, and were imaged at 10 \times objective on an optical microscope (Olympus, DP73, Tokyo, Japan). Only data from properly injected mice were used for statistical analyses.

Light-aversive test

For all behavioral testing, mice were acclimatized in their cages in the testing room for at least 2 h. To evaluate the typical migraine-associated photophobia induced by GTN, we used a modified light/dark box with infrared beam tracking (Shanghai Xinruan Information Technology Co., Ltd., XR-XB120, Shanghai, China). The box (30 cm wide×30 cm deep×30 cm high) consisted of two equally sized compartments: one painted white and brightly lit (1000 lx) with an LED panel, the other painted black and not lit (<5 lx). A corridor (7 cm×7 cm) connected the two compartments and allowed the mice to move freely. Light-aversive behaviors were examined in different batches of mice separately during the early (50–70 min) and late phases (110–130 min) after GTN/VEH injection (Fig. 1), according to previous studies [39, 40]. Each mouse was gently placed in the center of the light zone, facing away from the dark side. Between animals, the box was thoroughly cleaned using 75% alcohol.

All data were recorded and analyzed using a SuperMaze video-tracking system (Shanghai Xinruan Information Technology Co., Ltd., XR-Xmaze, Shanghai, China). We excluded mice who were inactive for 90% or more of the testing time. Decreased transitions and time spent in light were considered to reflect light-aversion behaviors.

von Frey Test

Cutaneous allodynia is a form of sensory amplification that occurs during a migraine attack. Consequently, facial and hind paw mechanical allodynia were quantified using calibrated von Frey filaments (Aesthesio[®], Danmic Global, San Jose, CA, USA). To test head thresholds, the hair on the mice's foreheads (above and between two eyes) was shaved, and mice were handled extensively for at least 3 days before testing for 5 min per day. On the test day, the experimenter gently held the mouse on the palm with minimal restraint and a series of calibrated von Frey filaments were perpendicularly applied to the shaved skin, causing the filaments to bend for 3 s. As previously described [41], criteria for a positive response included the mouse vigorously stroked face with the forepaw, head withdrawal, or head shaking. For hind paw testing, mice were placed in plexiglass chambers (10 cm

wide×7 cm deep×16 cm high), one mouse per chamber, on a mesh floor to acclimate for 30 min during each of the 3 days before testing. The plantar surface of the left hind paw was stimulated with von Frey filaments until a withdrawal of the paw or paw licking occurred.

We used the up-down method [42], where, if the animal produced a negative response, the researchers applied the filament with the next-greater force. If the animal produced a positive response, the stimulus was decreased. After the first breaking point (change in response), four more stimulations were applied, the response pattern and final filament were noted, and 50% withdrawal thresholds were calculated using a freely available online algorithm at https://bioapps.shinyapps.io/von_frey_app/ [43].

We determined the 50% hind paw and head withdrawal thresholds before injection (baseline) and 0.5, 1, 1.5, 2, 2.5, 3, 4, and 5 h after GTN/VEH injection in Fig. 1.

Elevated Plus Maze (EPM) test

Anxiety-like behaviors related to migraine were evaluated using an elevated plus maze (EPM; Shanghai Xinruan Information Technology Co., Ltd., XR-XG201, Shanghai, China). The EPM consisted of two open (35 cm wide×5 cm deep, 60 lx) and two closed arms (35 cm wide×5 cm deep×15 cm high, <5 lx) connected by a central platform (5 cm wide×5 cm deep), forming a plus. The maze was elevated 60 cm from the floor. Mice were placed in the central platform facing an open arm and were allowed to freely explore the EPM for 10 min. The maze was thoroughly cleaned with 75% alcohol between mice. Movements were tracked and analyzed with SuperMaze software (Shanghai Xinruan Information Technology Co., Ltd., XR-Xmaze, Shanghai, China). Time spent in open/closed arms and the number of open/closed-arm entries were determined by the software.

EPM test was performed in different batches of mice separately at 2, 4, and 24 h after GTN/VEH injection in Fig. 2.

Whole-brain imaging and image processing

Since NPY is widely distributed throughout the central nervous system, we performed whole-brain mapping of NPY expression in NPY-GFP mice with high-speed and high-throughput Volumetric Imaging with Synchronized

(See figure on next page.)

Fig. 1 Acute glyceryl trinitrate (GTN) administration produces transient allodynia and photophobia. **A** The schematic illustration of the von Frey test indicates the region where the von Frey stimulus was applied during testing. **B** and **C** Time course of GTN-induced changes in left hind paw (**B**) and head withdrawal thresholds (**C**) based on von Frey tests. **D** and **G** Example traces of mice in 20-min light-aversive test at 1 h (**D**) and 2 h (**G**) after VEH or GTN injection. **E** and **H** Average time spent in light for each group per 5-min interval (left panel) and over a total of 20 min (right panel) at 1 h (**E**) and 2 h (**H**) after VEH or GTN injection. **F** and **I** The number of transitions between zones expressed as the average for each group per 5-min interval (left panel) and during a total of 20 min (right panel) at 1 h (**F**) and 2 h (**I**) after VEH or GTN injection. $n=9$ mice per group. Significance was assessed by two-way repeated-measures ANOVA with post hoc comparison between groups (B, C, E left panel, F left panel, H left panel, and I left panel) or by two-tailed unpaired Student's *t*-test (E right panel, F right panel, H right panel, and I right panel). All data are presented as the mean \pm S.E.M.

* $P < 0.05$, ** $P < 0.01$, *** $P < 0.001$

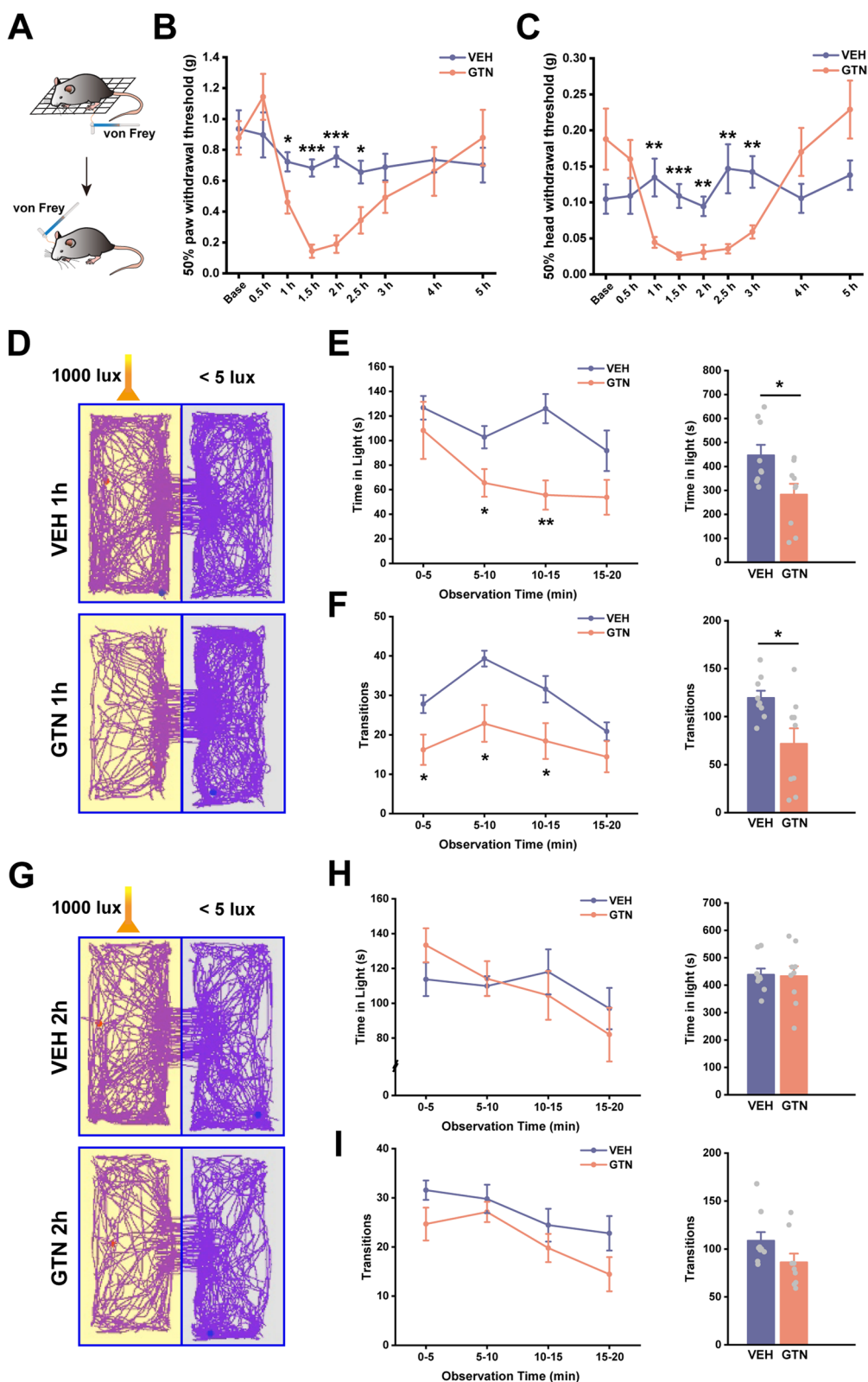


Fig. 1 (See legend on previous page.)

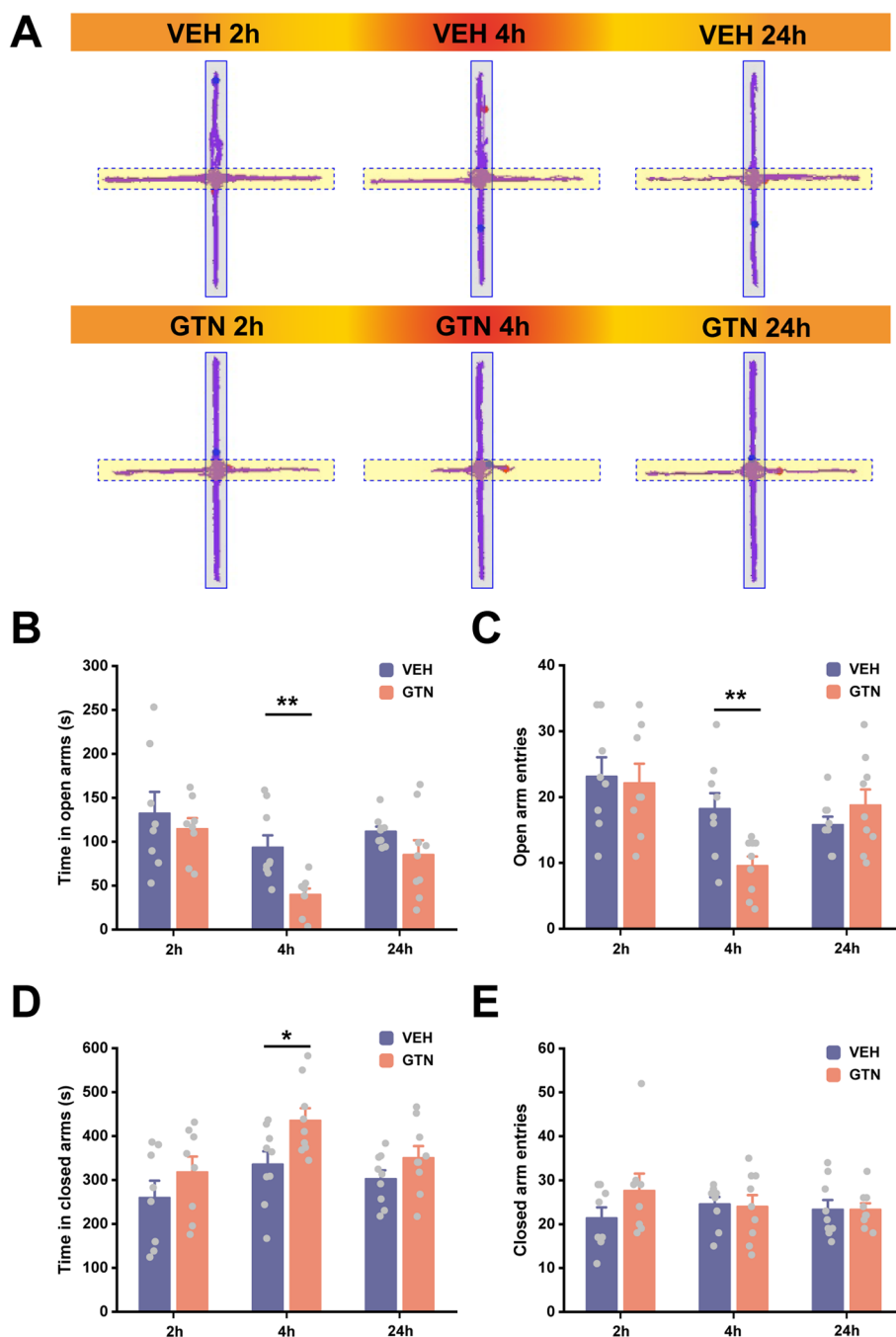


Fig. 2 Acute glyceryl trinitrate (GTN) administration induces delayed occurrence of anxiety-like behaviors. **A** Representative traces of mice in 10-min Elevated Plus Maze (EPM) test at 2 h, 4 h, and 24 h after VEH or GTN injection. **B-E** Time spent in the open arms (**B**), the number of open arm entries (**C**), time spent in the closed arms (**D**), and the number of closed-arm entries (**E**) during the EPM test at 2 h ($n=8$ mice per group), 4 h ($n=9$ mice per group), and 24 h ($n=9$ mice per group) after VEH or GTN injection. Significance was assessed by a two-tailed unpaired Student’s t-test. All data are presented as the mean \pm S.E.M. * $P < 0.05$, ** $P < 0.01$

on-the-fly-scan and Readout (VISoR), as previously described [44]. Two hours after intraperitoneal (i.p.) injection of GTN or VEH, the mice were deeply anesthetized with 1.5% Avertin and transcardially perfused with

20 ml of 0.1 M phosphate-buffered saline (PBS, pH 7.4) at 37 °C and 4 °C, respectively, followed by 20 ml of ice-cold 4% (wt/vol) paraformaldehyde (PFA) in PBS. Then brains were carefully removed and post-fixed in 4% PFA for 24 h

at 4°C. Next, the brains were transferred into 4% hydrogel monomer solution (HMS, 4% acrylamide, 0.05% bis-acrylamide, 4% PFA, and 0.25% VA-044 thermal initiator in PBS (wt/vol)) for 2 days at 4 °C, allowing penetration of fixation solution. Then, the samples were embedded in an equal volume mixture of 20% bovine albumin serum and 4% HMS for 4 h at 37 °C, followed by three washes (2 h each) with room-temperature PBS.

The embedded samples were sectioned into 300- μm consecutive coronal slices using a vibrating microtome (Compresstome VF-300, Precisionary Instruments, Greenville, NC, USA). The brain slices were cleared in 5% (vol/vol) PBST (5% Triton X-100 in PBS) with gentle shaking for 24 h at 37 °C, then rinsed in PBS three times (8 h each).

Lastly, the brain slices were mounted on glass slides in sequence and were polymerized with 4% HMS for 4 h at 37 °C. After three rinses with PBS, the slides were immersed overnight in a refractive-index-matching solution (80% iohexol in PBS (wt/vol)) with a refractive index of 1.52.

All slices were imaged with a custom VISoR microscope at $1 \times 1 \times 2.5 \mu\text{m}^3$ voxel resolution and stitched together to automatically reconstruct the whole mouse brain volume using custom-developed algorithms and software [44]. To identify the specific brain regions, the images were down sampled to $4 \times 4 \times 4 \mu\text{m}^3$ resolution and registered to the Allen Mouse Brain Common Coordinate Framework (Allen CCF) [45] using custom software.

For NPY cell counting, the images of $4 \times 4 \times 4 \mu\text{m}^3$ resolution were stacked to images of 25 μm in the Z direction with ImageJ. Cell counting was first trained manually to identify and count the neurons within 40 representative, 25- μm images using Ilastik software (version 1.3.3post3, University of Heidelberg, Heidelberg, Germany). Then, all of these 25- μm images were automatically processed in batches. Finally, we matched the positions of NPY neurons to the Allen CCF using custom software to determine the number of neurons within each brain area.

Immunofluorescence staining and imaging

To evaluate the expression levels of NPY Y1 receptor and Y2 receptor in the MHb, we performed immunofluorescence staining in C57BL/6 J mice. The perfusion process was the same as that for VISoR imaging. After post-fixation, brains were subsequently infiltrated with 15% (wt/vol) and 30% (wt/vol) sucrose sequentially until they sank to the bottom, embedded in O.C.T. TissueTek Compound (Sakura Finetek, 4583, Torrance, CA, USA), and then sectioned into 30- μm coronal slices using a freezing microtome (Leica Biosystems, CM1950, Heidelberg, Germany), after which they were stored in PBS.

Free-floating sections were incubated with a blocking buffer containing 10% (vol/vol) normal donkey serum and 0.25% (vol/vol) Triton X-100 dissolved in PBS for 1.5 h at room-temperature. The sections were then incubated overnight at 4°C with primary rabbit anti-Y1 receptor (1: 500, Neuromics, RA24506, Edina, MN, USA) or rabbit anti-Y2 receptor (1: 500, Neuromics, RA14112, Edina, MN, USA) diluted in blocking buffer. Next, sections were washed 3 times (20 min each) with 0.25% PBST (0.25% Triton X-100 in PBS) and incubated with a fluorescent dye-conjugated donkey anti-rabbit secondary antibody (1:1000, Abcam, ab150061, Waltham, MA, USA) for 2 h at room-temperature. Following three washes (20 min each) with PBST, sections were mounted and coverslipped with mounting medium with DAPI (Abcam, ab104139, Waltham, MA, USA).

Fluorescence images were acquired as z-stacks (2 μm step size for 20 μm per stack) using a panoramic confocal scanner (3DHISTECH Ltd., Budapest, Hungary) with a 20 \times , 0.8 NA objective. Six sections were selected from the MHb (from 1.06–2.06 mm posterior to bregma) for each receptor from an individual animal. Intensity quantifications were performed using ImageJ software (Fiji, NIH, USA). Based on reports in related literature, the sample size was not predetermined by calculation.

Statistical analysis

All experiments and data analyses were conducted by experimenters blinded to group assignment. Sample sizes were determined by previous experience, and all were numbers of biological repeats. Data are shown as mean \pm standard error of the mean (S.E.M.). Two-tailed unpaired Student's t-test, one-way ANOVA, two-way ANOVA, two-way repeated-measures ANOVA, and Kruskal–Wallis H test were performed using SPSS version 22 (IBM Analytics, Armonk, NY, USA). Details of each analysis are included in the figure legends and statistical significance was set at $P < 0.05$.

Results

Phenotypic characterization of the GTN-induced migraine model in mice

Although the GTN mouse model is well validated by its induction of migraine-like headaches and response to specific migraine drugs [46, 47], researchers rarely investigated non-headache symptoms in a time-dependent manner. To investigate the impact of GTN on both sensory and affective aspects of migraine-like behaviors, we treated male C57BL/6 J mice with GTN or vehicle (VEH) and tested them for generalized allodynia, photophobia, and anxiety-like behaviors. As shown in Fig. 1A–C, mice administered with GTN displayed a time-dependent decrease in mechanical withdrawal thresholds of the hind

paw (time×group interaction: $F(3.490, 55.835)=5.106$, $P=0.002$; simple effects: 1 h: $F(1, 16)=6.667$, $P=0.020$; 1.5 h: $F(1, 16)=52.122$, $P<0.001$; 2 h: $F(1, 16)=38.362$, $P<0.001$; 4 h: $F(1, 16)=0.161$, $P=0.694$) as well as the head (time×group interaction: $F(4.143, 66.296)=7.197$, $P<0.001$; simple effects: 1 h: $F(1, 16)=9.585$, $P=0.007$; 1.5 h: $F(1, 16)=20.567$, $P<0.001$; 2 h: $F(1, 16)=12.829$, $P=0.002$; 4 h: $F(1, 16)=2.435$, $P=0.138$) relative to VEH-treated mice. These effects developed within 1 h and reached their lowest levels at 1.5 h. Mechanical hypersensitivity had recovered gradually at 2 h, then subsided at 4 h after GTN administration.

Besides allodynia, we evaluated light-aversive behaviors (photophobia) using a modified light/dark box. Within the first 50 min after GTN injection, the mice showed remarkable reductions in locomotor activity due to the cardiovascular effects (hypotension) of GTN [48]. Consequently, these mice were inactive for more than 90% of the time spent in the box (data not shown). Because of this, we performed the light-aversion test at 1 h (early phase) and 2 h (late phase) after GTN administration. The durations comprised four intervals of 5 min each. Firstly, in the early phases after drug injection, GTN mice spent significantly less time in the light compared with VEH mice during the total 20 min (Fig. 1E right panel; $t(2, 16)=2.633$, $P=0.018$), especially at the 5–10 min and 10–15 min intervals (Fig. 1E left panel; time×group interaction: $F(1.800, 28.793)=1.674$, $P=0.207$; time: $F(1.800, 28.793)=5.195$, $P=0.014$; group: $F(1, 16)=6.932$, $P=0.018$; 5–10 min interval: $F(1, 16)=5.865$, $P=0.028$; 10–15 min interval: $F(1, 16)=15.526$, $P=0.001$). We further analyzed the number of transitions between the light and dark chambers as an indicator of light-aversive behavior. Compared to VEH mice, GTN-treated mice transitioned less at 0–5 min, 5–10 min, and 10–15 min intervals (Fig. 1F left panel; time×group interaction: $F(3, 48)=1.549$, $P=0.214$; time: $F(3, 48)=11.402$, $P<0.001$; group: $F(1, 16)=7.310$, $P=0.016$; 0–5 min interval: $F(1, 16)=5.909$, $P=0.030$; 5–10 min interval: $F(1, 16)=9.411$, $P=0.011$; 10–15 min interval: $F(1, 16)=4.774$, $P=0.044$) as well as during the total 20 min (Fig. 1F right panel; $t(2, 11.159)=2.704$, $P=0.020$). However, in the late phases, referred to as 2 h, GTN mice showed no signs of photophobia in both times in light and transitions (Fig. 1G–I; H left panel: time×group interaction: $F(3, 48)=1.049$, $P=0.380$; time: $F(3, 48)=3.166$, $P=0.033$; group: $F(1, 16)=0.012$, $P=0.913$; H right panel: $t(2, 16)=0.111$, $P=0.913$; I left panel: time×group interaction: $F(3, 48)=0.485$, $P=0.694$; time: $F(3, 48)=7.178$, $P<0.001$; group: $F(1, 16)=3.047$, $P=0.100$; I right panel: $t(2, 16)=1.746$, $P=0.100$).

Anxiety and mood disorders are the most frequent psychiatric migraine comorbidities [49]. Pre-clinical

studies reported anxiety-like behaviors, mainly in chronic migraine animal models [50, 51]. In this study, we quantified the degree of anxiety in an acute migraine mouse model induced by GTN with an EPM test. We found that a single GTN injection reduced the time spent in open arms and the number of open arm entries (Fig. 2A–C; B: $t(2, 11.797)=3.477$, $P=0.005$; C: $t(2, 16)=3.142$, $P=0.006$). Meanwhile, time in closed arms increased (Fig. 2D; $t(2, 16)=-2.466$, $P=0.025$) at 4 h after GTN application. Interestingly, no differences were observed at 2 h or 24 h (Fig. 2A–E), suggesting delayed anxiety after recovering from mechanical allodynia caused by GTN. Furthermore, there was no significant difference between the groups in the total distance travelled. This finding suggested that EPM test performance was not influenced by functional motor differences (Fig. S1). Taken together, these results demonstrated that acute GTN administration is an effective and reliable migraine model for triggering allodynia, photophobia, and anxiety-like behaviors in mice. We also determined the “best” timepoints for examination of different behaviors. More importantly, we revealed the evolutive sequence of symptoms induced by GTN. The observed sequences mimicked the symptom progression seen in patients who experience frequent migraine attacks.

GTN alters NPY expression in the MHB

NPY is widely distributed throughout the central nervous system. To identify the critical regions expressing NPY in the brain that may be responsible for the migraine-like phenotypes in the GTN mice, we used whole-brain VISoR imaging, as previously described by Wang et al. [44]. NPY-GFP reporter mice were subjected to GTN or VEH injection. Two hours later, brains from these mice were processed and imaged. The NPY levels were quantified using previously established counting methods. Representative images and the anatomic distribution of NPY neurons from VEH mice are shown in Fig. 3. Overall, NPY was highly expressed in the cerebral cortex (including neocortex, hippocampus, and olfactory bulb), striatum, thalamus (reticular nucleus of the thalamus, ventral posterior complex of the thalamus, habenula, and medial geniculate complex), hypothalamic nuclei (arcuate nucleus, paraventricular nucleus), superior colliculus sensory related, inferior colliculus, periaqueductal gray, and medulla (Fig. 3A, B).

While in response to GTN treatment, there were no significant differences in NPY neuron populations in some migraine-related brain areas, such as the spinal nucleus of the trigeminal caudal part (SPVC, $t(2, 10)=2.121$, $P=0.060$), ventral posteromedial nucleus of the thalamus (VPM), lateral posterior nucleus of the thalamus (LP), and nucleus of the solitary tract (NTS,

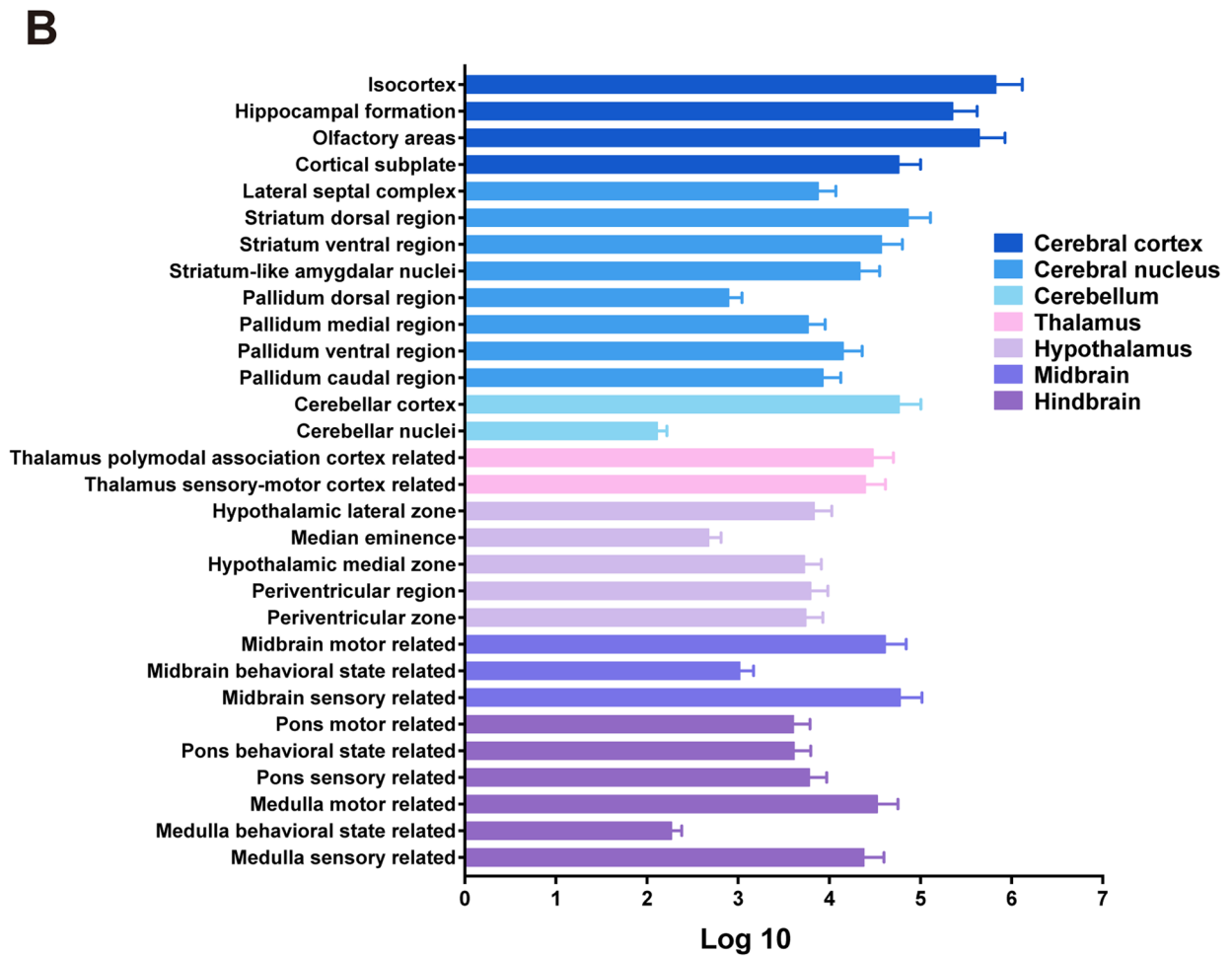
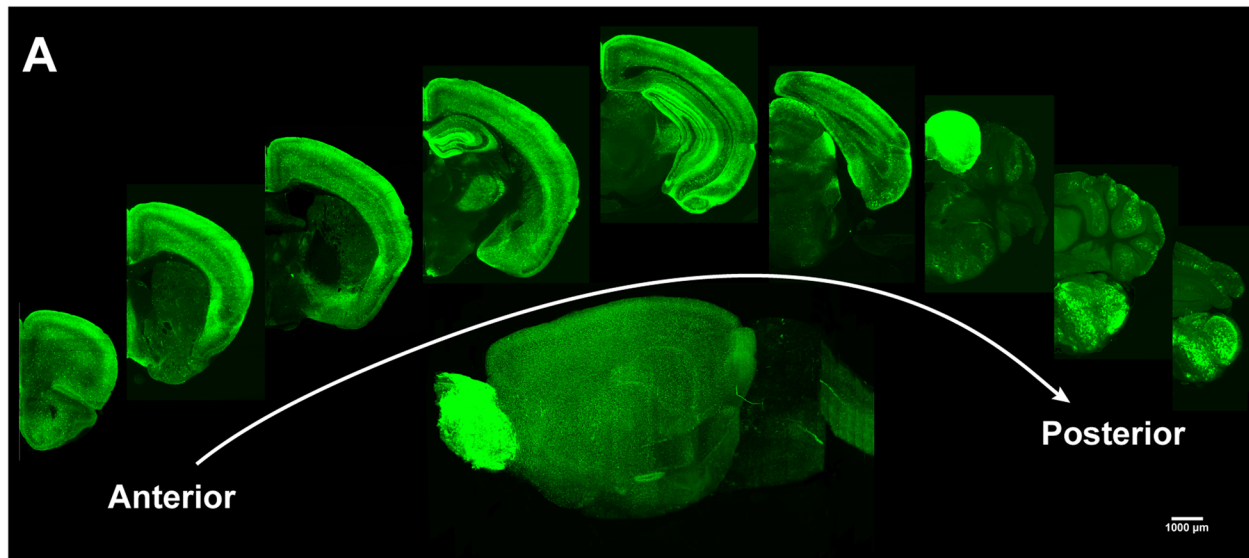


Fig. 3 VISoR imaging of NPY-GFP mice shows the distribution of NPY across the whole brain. **A** The representative reconstructed NPY (green) images from a VEH mouse brain (scale bar, 1000 μm). **B** Quantitative NPY neurons across the whole-brain areas from the VEH group. *n* = 6 mice per area

$t(2, 10)=0.776, P=0.456$). Importantly, we noted a statistically significant decrease in GFP⁺ cells in certain brain areas, including the medial habenula (MHb, $t(2, 10)=2.376, P=0.039$), spinal nucleus of the trigeminal oral part (SPVO, $t(2, 10)=2.421, P=0.036$), nucleus of the posterior commissure (NPC, $t(2, 10)=2.261, P=0.047$), and paragigantocellular reticular nucleus (PGRN, $t(2, 10)=2.266, P=0.047$) (Fig. 4A, B). Oppositely, compared with the VEH group, more GFP⁺ cells were found in the gustatory areas layer 5 (GU5, $t(2, 10)=-3.429, P=0.006$) and primary somatosensory area nose layer 5 (SSp-n5, $t(2, 10)=-2.608, P=0.026$) in GTN mice (Fig. 4A, B). Among them, the MHb is a key site for pain modulation and affective and motivational processes [52]. Given that the NPY is also a potent neuromodulator playing roles in analgesia and antianxiety effects, changed NPY expression in the MHb by GTN might be the cause of GTN-induced migraine-like phenotypes. The numbers of NPY neurons in other brain areas from VEH and GTN mice were presented in Table S1.

NPY signaling in the MHb alleviates GTN-induced allodynia and anxiety-like behaviors

To determine the role of MHb NPY in the development of allodynia, photophobia, and anxiety under GTN condition, we performed microinjection of NPY into the bilateral MHb immediately before GTN injection. Then, we sequentially tested light-aversive behaviors at 1 h, mechanical withdrawal thresholds at 1.5 h, and anxiety-like behaviors at 4 h after GTN injection. Control mice were injected with VEH+saline (Fig. 5A). A representative cannula location is shown in Fig. S4. Consistent with our results (Figs. 1 and 2), GTN+saline mice exhibited photophobia, allodynia, and anxiety-like behaviors compared to VEH+saline mice (Fig. 5B–H). However, NPY in the MHb had no influence on GTN-induced reductions in time-in-light and number of transitions in the light/dark box (Fig. 5B, C; B left panel: time×group interaction: $F(9, 117)=1.513, P=0.151$; time: $F(3, 117)=13.138, P<0.001$; group: $F(3, 39)=8.095, P<0.001$; 0–5 min interval: $F(3, 39)=1.437, P=0.247$; 5–10 min interval: $F(3, 39)=5.062, P=0.005$; 10–15 min interval: $F(3, 39)=5.662, P=0.003$;

15–20 min interval: $F(3, 39)=9.910, P<0.001$; B right panel: model×drug interaction: $F(1, 39)=0.456, P=0.504$; model: $F(1, 39)=22.352, P<0.001$; drug: $F(1, 39)=1.968, P=0.169$; C left panel: time×group interaction: $F(9, 117)=2.087, P=0.036$; simple effects: 0–5 min interval: $F(3, 39)=4.781, P=0.006$; 5–10 min interval: $F(3, 39)=4.065, P=0.013$; 10–15 min interval: $F(3, 39)=0.783, P=0.511$; 15–20 min interval: $F(3, 39)=1.975, P=0.134$; C right panel: model×drug interaction: $F(1, 39)=0.134, P=0.716$; model: $F(1, 39)=9.543, P=0.004$; drug: $F(1, 39)=0.106, P=0.746$). Strikingly, infusion of NPY robustly increased both hind paw (model×drug interaction: $F(1, 39)=5.739, P=0.021$; simple effects: $P=0.047$, GTN+saline versus GTN+NPY) and head withdrawal thresholds ($\chi^2(3)=17.053, P=0.001$; $U=23.000, P=0.024$, GTN+saline versus GTN+NPY), time spent in open arms (model×drug interaction: $F(1, 39)=22.491, P<0.001$; simple effects: $P=0.010$, GTN+saline versus GTN+NPY) and number of open arm entries (model×drug interaction: $F(1, 39)=19.663, P<0.001$; simple effects: $P=0.028$, GTN+saline versus GTN+NPY) and also consistently reduced time in closed arms (model×drug interaction: $F(1, 39)=9.681, P=0.003$; simple effects: $P=0.032$, GTN+saline versus GTN+NPY) in EPM compared to treatment with saline under the GTN paradigm (Fig. 5D–H). Unpredictably, VEH+NPY mice showed a significantly shorter time in open arms (model×drug interaction: $F(1, 39)=22.491, P<0.001$; simple effects: $P=0.001$, VEH+saline versus VEH+NPY) and fewer number of open arm entries (model×drug interaction: $F(1, 39)=19.663, P<0.001$; simple effects: $P=0.001$, VEH+saline versus VEH+NPY) in EPM, accompanied by a longer time in closed arms (model×drug interaction: $F(1, 39)=9.681, P=0.003$; simple effects: $P=0.035$, VEH+saline versus VEH+NPY), when compared to VEH+saline mice (Fig. 5F–H). Plus, no difference was found between groups in the total distance travelled in EPM (Fig. S2). Taken together, NPY in the MHb attenuated GTN-induced allodynia and anxiety without affecting photophobia, whereas microinjection of NPY in the VEH mice led to an increase in anxiety-like behavior.

(See figure on next page.)

Fig. 4 GTN alters NPY expression in several brain areas, including the medial habenula (MHb). **A** The representative reconstructed NPY (green) images from a VEH or GTN mouse brain in diverse brain areas. Each group's left panel is the overview (scale bar, 1000 μ m), and higher magnification close-ups are shown in the right panel (scale bar, 100 μ m). The white contour delineates the borders of the respective brain areas. **B** Summary fold changes in the number of NPY neurons of the GTN group over the VEH group in multiple brain areas. $n=6$ mice per group. Significance was assessed using a two-tailed unpaired Student's t-test. Data are presented as the mean \pm S.E.M. * $P<0.05$, ** $P<0.01$. MHb, medial habenula; SPVO, spinal nucleus of the trigeminal oral part; SPVC, spinal nucleus of the trigeminal caudal part; GU5, gustatory areas layer 5; SSp-n5, primary somatosensory area nose layer 5; SSp, primary somatosensory area; SSS, supplemental somatosensory area; VPM, ventral posteromedial nucleus of the thalamus; LP, lateral posterior nucleus of the thalamus; NPC, nucleus of the posterior commissure; PGRN, paragigantocellular reticular nucleus; NTS, nucleus of the solitary tract

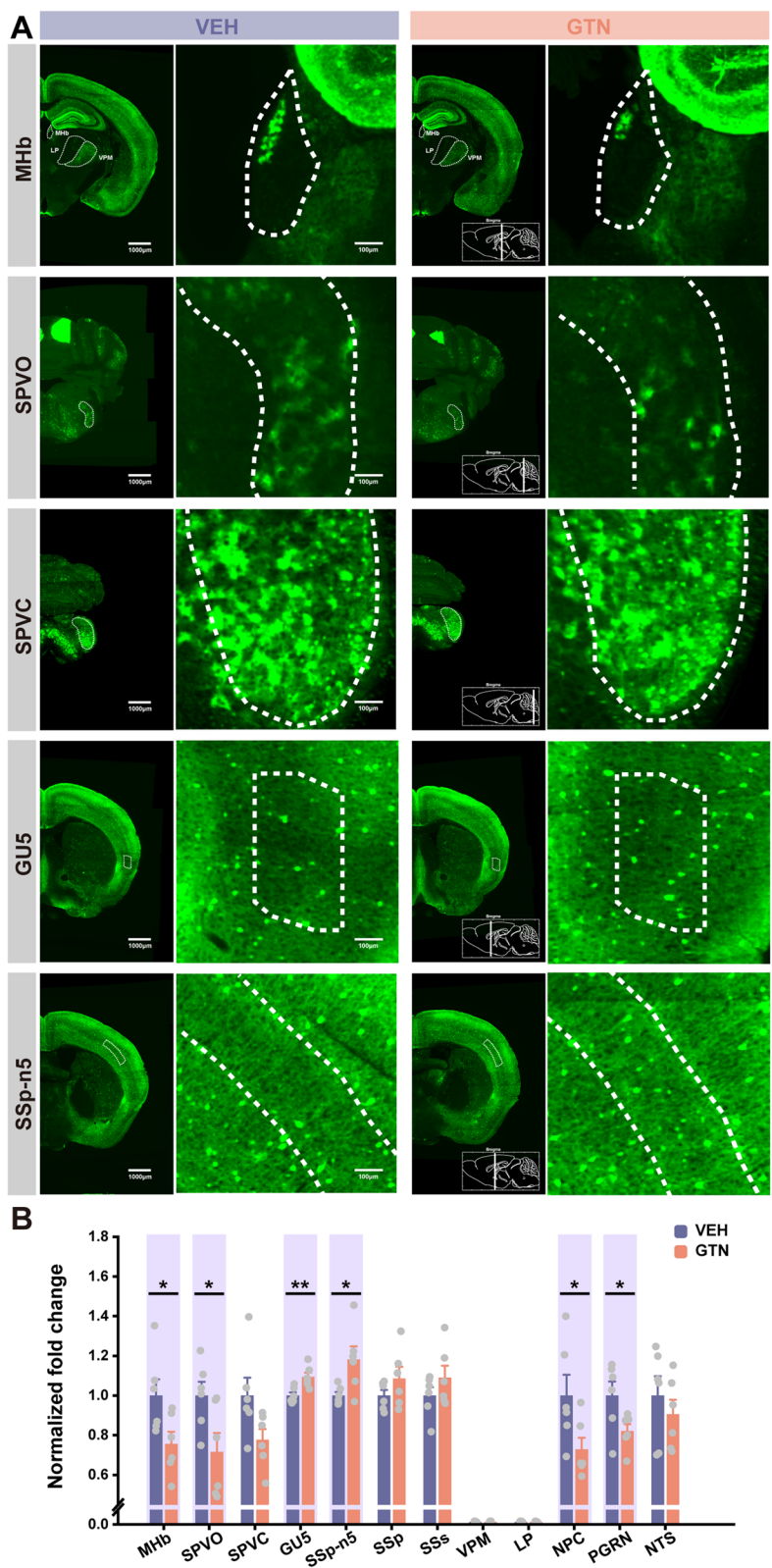


Fig. 4 (See legend on previous page.)

NPY signaling in the MHb exerts its analgesic and anxiolytic effects through the Y1 receptor in GTN mice

NPY acts via at least five different Y receptors in mice, of which the Y1 and Y2 receptors are the most abundant and intensively investigated in studies of nociception [53–55]. Importantly, the Y1 receptor has also been demonstrated to be involved in NPY-mediated anxiolytic effects [16, 56]. Hence, to obtain more insights into our results, we explored the protein expressions of the two major NPY receptors—Y1 and Y2 receptors in the MHb—by fluorescent staining. We first confirmed that there were Y1 and Y2 receptors expressed in the MHb (Fig. 6A, B). Secondly, the expression of the Y1 receptor was remarkably increased by GTN (Fig. 6A; $t(2, 6) = -4.255$, $P = 0.005$), while no difference was found in Y2 receptor expression between VEH and GTN mice (Fig. 6B; $t(2, 6) = -1.037$, $P = 0.340$). These findings suggest that the Y1 receptor may mediate the effects of NPY in the MHb.

Given the fact that the administration of NPY per se cannot discriminate which receptor pathways were activated, we then repeated the MHb microinjection experiment using Y1 and Y2 receptor agonists, respectively. Interestingly, as shown in Fig. 7A, activation of both Y1 and Y2 receptor signaling pathways in GTN mice significantly increased hind paw withdrawal thresholds, with a more profound effect by Y1 receptor agonist ($\chi^2(2) = 15.045$, $P = 0.001$; $U = 6.000$, $P < 0.001$, GTN+saline versus GTN+Y1R agonist; $U = 22.000$, $P = 0.020$, GTN+saline versus GTN+Y2R agonist). As for head allodynia, only GTN+Y1R agonist mice showed prominent alleviation of mechanical pain hypersensitivity compared to GTN+saline mice; we found no difference between GTN+Y2R agonist and GTN+saline mice in head pain hypersensitivity (Fig. 7B; $\chi^2(2) = 6.341$, $P = 0.042$; $U = 22.000$, $P = 0.020$, GTN+saline versus GTN+Y1R agonist; $U = 28.000$, $P = 0.061$, GTN+saline versus GTN+Y2R agonist). Moreover, activating the MHb Y1 receptor increased the time spent in open arms in the EPM test ($F(2, 29) = 4.297$, $P = 0.023$; post hoc comparison: $P = 0.013$), accompanied by less time in closed arms (Fig. 7C, E). Despite these differences, we did not observe any changes in the frequency entering open or

closed arms (Fig. 7D, F). On the contrary, activating the Y2 receptor seemingly induced anxiety-like behaviors, as indicated by an increased number of closed-arm entries (Fig. 7E; $F(2, 29) = 5.280$, $P = 0.011$; post hoc comparison: $P = 0.004$). However, the time spent in open and closed arms and the frequency of open-arms entry were not affected by the Y2 receptor agonist (Fig. 7C–E). Finally, the motor abilities in EPM of all groups were similar, proved by the results of total distance travelled (Fig. S3). Together, these results indicate the MHb Y1 receptor is predominantly involved in relieving allodynia and anxiety-like behaviors induced by GTN.

Discussion

Migraine is a common headache disorder with heterogeneous symptoms. In this study, we confirmed the allodynia, photophobia, and anxiety-like behaviors accompanied migraine. We also determined the timing of effects induced by acute GTN administration; these results provided the experimental basis for our research. Next, we generated a clear NPY expression map of the whole brain for the first time, and found considerable changes in NPY levels in select brain areas in GTN mice. These results will undoubtedly inform future studies. Finally, we initiatively identified the key role of MHb NPY in the alleviation of allodynia and anxiety-like behaviors through the Y1 receptor in the GTN-induced migraine model.

NPY is involved in migraine pathogenesis. Although Oliveira et al. [57] demonstrated that NPY reduced trigeminocervical complex neuronal firing through the Y1 receptor in a migraine rat model, NPY was applied systemically, meaning that it may potentially affect the entire neural network. Till date, the specific roles of NPY in migraine and how it functions after migraine onset remain unclear. Therefore, we must determine how NPY levels are altered following GTN administration. Unfortunately, studies that examined NPY changes in patients with migraine produced highly variable findings [18–20]. This variability may reflect trial design and study cohort differences. A recent preclinical study reported on dynamic changes in NPY using a rat model where

(See figure on next page.)

Fig. 5 Microinjection of NPY into the MHb alleviates GTN-induced allodynia and anxiety-like behaviors. **A** Plan of the experimental procedure: MHb microinjections were performed immediately before VEH or GTN injection. **B** and **C** Effects of NPY or saline on time spent in light (**B**) and the number of transitions between zones (**C**) expressed as the average for each group per 5-min interval (left panel) and during a total of 20 min (right panel) in a light-averse test at 1 h after VEH or GTN injection. **D** and **E** Effects of NPY or saline on the left hind paw (**D**) and head withdrawal thresholds (**E**) during the von Frey test at 1.5 h after VEH or GTN injection. **F–I** Effects of NPY or saline on time spent in the open arms (**F**), the number of open arm entries (**G**), time spent in the closed arms (**H**), and the number of closed arm entries (**I**) during the EPM test at 4 h after VEH or GTN injection. VEH+saline, $n = 11$ mice; GTN+saline, $n = 10$ mice; VEH+NPY, $n = 11$ mice; GTN+NPY, $n = 11$ mice. Significance was assessed by two-way repeated-measures ANOVA with post hoc comparison between groups (B and C left panel; * $P < 0.05$, ** $P < 0.01$, *** $P < 0.001$ VEH+saline versus GTN+saline; # $P < 0.05$, ## $P < 0.01$ VEH+NPY versus GTN+NPY) or by two-way ANOVA with post hoc comparison between groups (B and C right panel, D, F–I; * $P < 0.05$, ** $P < 0.01$, *** $P < 0.001$) or by Kruskal–Wallis H test with Mann–Whitney U post hoc comparison between groups (E; * $P < 0.05$, ** $P < 0.01$). All data are presented as the mean \pm S.E.M

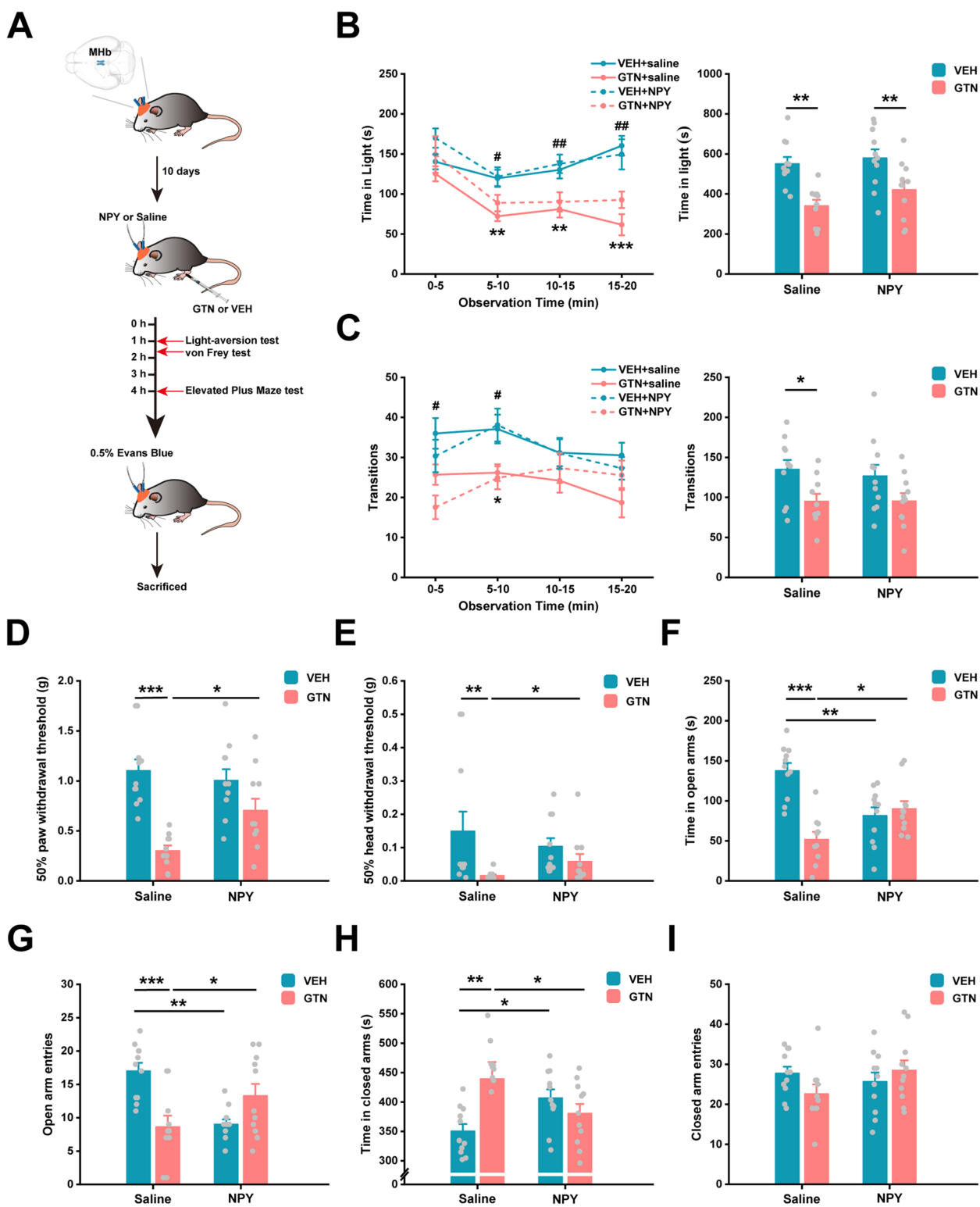


Fig. 5 (See legend on previous page.)

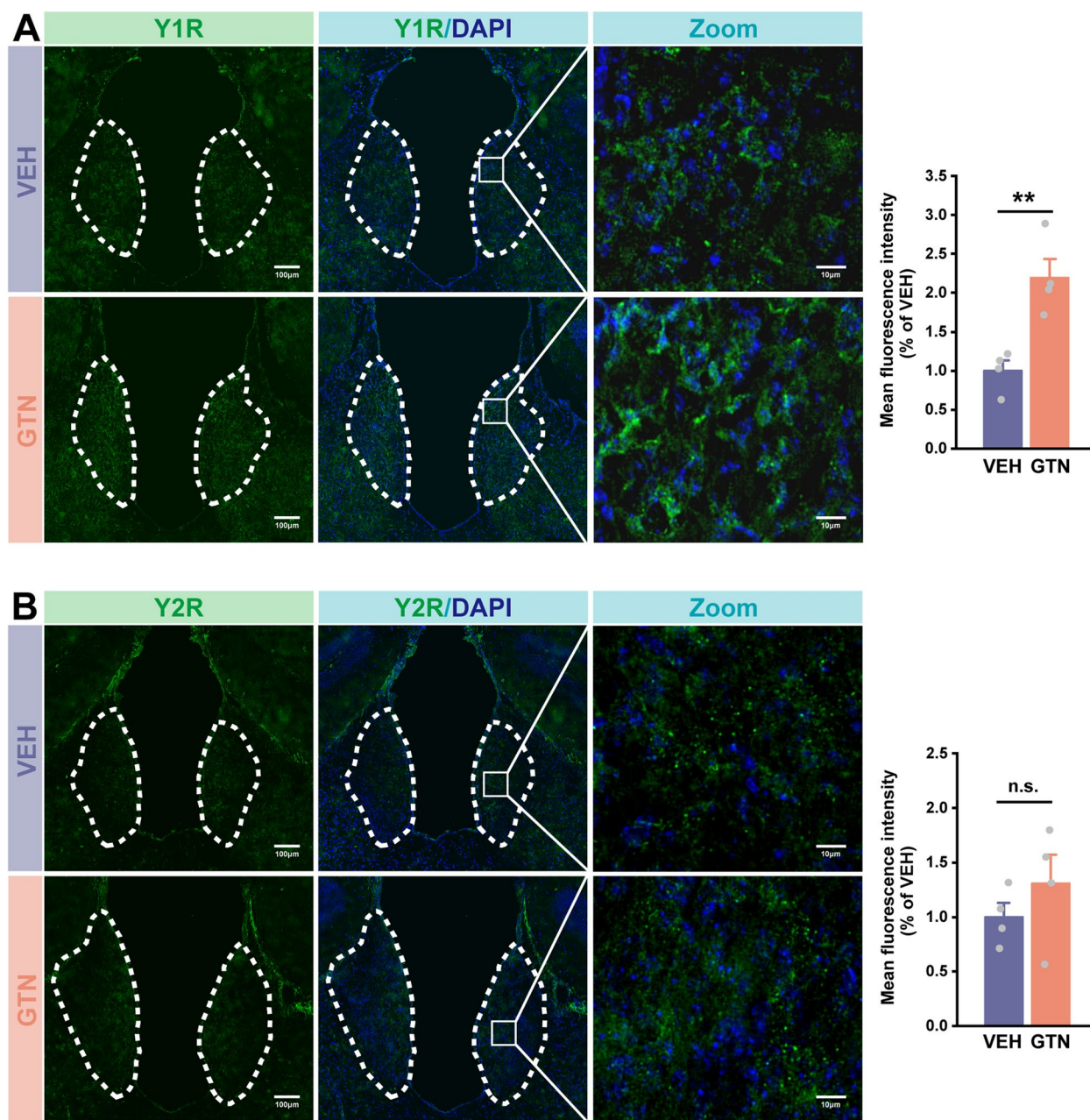


Fig. 6 GTN increases the expression of the Y1 receptor in the MHB, but not affects the Y2 receptor. **A** and **B** Left: representative images of Y1 receptor (**A**, green), Y2 receptor (**B**, green), and DAPI (blue) immunofluorescence of VEH and GTN mice. (scale bars: 100 μ m for overviews; 10 μ m for zooms). Right: mean fluorescence intensity of Y1 receptor (**A**) and Y2 receptor (**B**) in the GTN group relative to the VEH group. $n=4$ mice per group, six sections per mouse. Significance was assessed by a two-tailed unpaired Student's *t*-test. All data are presented as the mean \pm S.E.M. ****** $P < 0.01$

migraine was induced by electrical stimulation of the trigeminal ganglia (TG). Here, NPY expression was significantly elevated immediately after stimulation in TG and at 12 h in the blood plasma. Further elevations were observed upon repeated stimulation [58], confirming the important role of NPY in migraine pathogenesis. Unlike previous research, in the current study, we determined

whole-brain NPY expression levels using VISoR imaging and a well-accepted migraine mouse model. Our results revealed significant and early changes in NPY levels in the MHB, SPVO, NPC, PGRN, GU5, and SSp-n5 following GTN administration.

The MHB is a small, complex, and evolutionarily conserved structure located on the dorsal surface of the

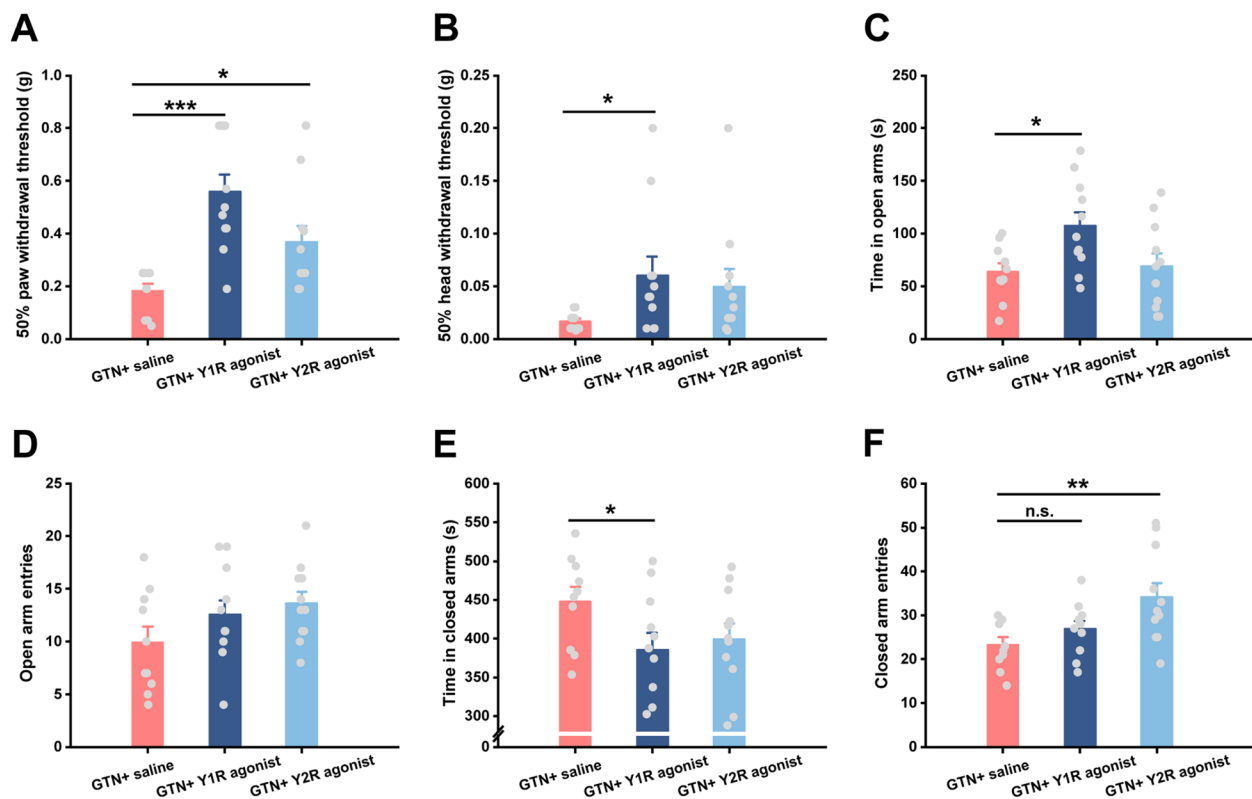


Fig. 7 Microinjection of Y1 receptor agonist into the MHB alleviates GTN-induced allodynia and anxiety-like behaviors. **A** and **B** Effects of the Y1 receptor agonist or Y2 receptor agonist on the left hind paw (**A**) and head withdrawal thresholds (**B**) in the von Frey test at 1.5 h after VEH or GTN injection. **C–F** Effects of the Y1 receptor agonist or Y2 receptor agonist on time spent in the open arms (**C**), the number of open arm entries (**D**), time spent in the closed arms (**E**), and the number of closed-arm entries (**F**) during the EPM test at 4 h after VEH or GTN injection. GTN + saline, $n = 10$ mice; GTN + Y1 receptor agonist, $n = 11$ mice; GTN + Y2 receptor agonist, $n = 11$ mice. Significance was assessed by Kruskal–Wallis H test with Mann–Whitney U post hoc comparison between groups (A and B; $*P < 0.05$, $***P < 0.001$) or by one-way ANOVA with post hoc comparison between groups (C–F; $*P < 0.05$, $**P < 0.01$). All data are presented as the mean \pm S.E.M

thalamus (epithalamus) and linking forebrain areas with midbrain monoaminergic centers [59, 60]. Although the MHB is somewhat neglected, there is increasing evidence of its important roles in pain [61], anxiety [62], depression [63], fear [64], and nicotine addiction behaviors [65]. The MHB acts as a major point of convergence where external stimuli are received, evaluated, and redirected to generate appropriate behaviors. Therefore, the fact that GTN mice showed photophobia, allodynia, and anxiety-like behaviors prompted us to further investigate reductions of NPY in the MHB using a mouse migraine model.

It has been demonstrated that NPY signaling inhibited pain in the PAG, PBN, trigeminal nucleus, and the dorsal horn of the spinal cord [57, 66–68]. The intracellular signaling mechanism in spine was previously elucidated. Briefly, NPY binds to the Gi-coupled Y1 receptor at key sites of pain transmission, inhibiting AC1 and intracellular signaling. Additionally, Y1R neurons hyperpolarize due to the opening of gated inwardly rectifying potassium channels (GIRK) and potassium influx following Gi

activation. Thus, NPY exerts analgesic effects [55]. Here, our findings uncover that the MHB acts as an additional action site for NPY’s analgesic effects and uniquely inhibits GTN-induced migraine-like pain. Clinical and preclinical studies have revealed the involvement of the habenula in pain. Shelton and co-workers [69] showed bilateral habenula activation during noxious heat stimulation with high-field magnetic resonance imaging (fMRI); thus, the habenula appears involved in sensory processing. Deep brain stimulation in the habenula revealed pain to be one of the most common transient effects of increased voltage [70]. However, due to its small size, current MRI techniques (3 T scanners) do not allow us to distinguish MHB from LHb signals. Meanwhile, 7 T scanners seem capable of separating signals from MHB and LHb in ex-vivo brains, but not functionally in vivo [71, 72]. Because of this, rodent studies of MHB are more reliable. A recent preclinical study reported distinct activation patterns within the MHB under a neuropathic pain condition [73]; meanwhile, lesioning the MHB increased pain

sensitivity [74]. Darcq et al. [61] reported that morphine acted through mu-opioid receptors directly on MHB neurons to produce analgesia. These data demonstrate that the MHB plays a role in direct analgesia through opioidergic systems. Given the high mu-opioid receptor density found in the MHB [75, 76], Y1 receptors in the MHB likely interact with opioidergic systems to produce analgesic effect. Alternatively, NPY signaling may also act as a novel neurotransmitter system and exert dependent nociception control. Several lines of evidence support the latter notion. Firstly, the intracellular mechanisms of signal transduction activated by NPY through Y1 receptors in spine have been reported to contribute to pain inhibition. Additionally, the presence of NPY and Y1 receptor has been proved in this structure by previous studies [77, 78] and our results, implying the direct analgesic effects of NPY signaling. Secondly, NPY Y1 and opioid receptors are Go/Gi-coupled receptors [61] and can activate the extracellular signal-regulated kinases (ERK1/2) [79]. Darcq et al. found that RSK2 signaling—a direct downstream effector of ERK1/2—contributed to acute morphine analgesia in the MHB. Thus, we speculate that NPY Y1 receptor-RSK2 signaling may directly mediate NPY's analgesic effects. Thirdly, the MHB primarily projects to the interpeduncular nucleus (IPN), co-releasing acetylcholine and glutamate. As a downstream structure of the MHB-IPN axis, the dorsal nucleus raphe receives GABAergic projection from IPN [80]. Thereby, the NPY Y1 receptor signaling may activate descending antinociceptive pathways (brainstem modulatory systems) by reducing neuron activity in the MHB. Further studies are needed.

Furthermore, we found mild differences in the analgesic effects functioned by Y1 and Y2 receptors (Fig. 7A, B). Although cutaneous allodynia is associated with central sensitization and synaptic plasticity [81], there is a specific difference in the underlying mechanisms between head allodynia and paw allodynia. Sandkühler and Gruber-Schoffnegger [82] reviewed that allodynia in stimulated region is attributed to homosynaptic long-term potentiation (potentiation of the same synapses that were stimulated), whereas allodynia beyond the stimulated territory may be caused by heterosynaptic potentiation (potentiation of non-stimulated synapses on the same cell) occurs in both principal cells and interneurons of the dorsal horn in limb pain models. Similar processes may occur in the MHB in GTN-induced migraine model, which could explain our results that paw allodynia was alleviated by both Y1 and Y2 agonists, but head allodynia was suppressed only by Y1 agonists. The more abundant expression of Y1 receptor in the MHB (Fig. 6) and the different distribution patterns of the two receptors at the synapses may

contribute to their functional differences in allodynia. The mechanisms will be further investigated.

In addition, there was a notable anxiolytic action of NPY and Y1R agonist, microinjected into the MHB, as evidenced by EPM. Previous works have demonstrated the anxiolytic effect of NPY acting at the Y1 receptor in other brain areas, including the amygdala, PAG, hippocampus, and lateral septum [83–85]. These effects are, in part, due to antagonism of stress-promoting signals such as corticotrophin-releasing factor [16, 86]. Although there are limited studies on the role of the MHB in anxiety in humans, many preclinical studies found the MHB to be a powerful modulator of anxiety-like behaviors. Early lesion and pharmacological studies have implicated the habenular pathway in anxiety-related behaviors in rodents [87–89]. These studies, however, did not identify the precise neural mechanisms underlying observed negative emotional behaviors due to technical limitations. Using the genetic tools, Yamaguchi et al. [62] demonstrated that TS→ventral MHB→IPN neural transmission was crucial for anxiety; ablation of this pathway reduced anxiety-related behaviors. Similarly, Pang et al. [90] expressed novel nAChR subunits selectively in MHB cholinergic neurons of adult mice, which was able to activate MHB cholinergic neurons, and found that the agonist of nAChR subunits increased anxiety levels. Thus, MHB cholinergic signaling appears important for modulating anxiety-like responses, with increased activity of MHB cholinergic neurons being associated with a heightened anxiety-like state, while the decreased activity of MHB cholinergic neurons being linked with decreased anxiety [91]. In line with these findings, in this study, we observed that NPY attenuated anxiety-like behaviors induced by GTN in the MHB; this at least partly attributed to the inhibitory effects of NPY on cholinergic neurons through the Y1 receptor. On the contrary, it is worth noting that some researches indicated that activation—but not inhibition—of MHB cholinergic signaling remarkably suppressed anxiety-like behaviors. For example, mice deprived of MHB neurons postnatally exhibited mildly increased anxiety levels [92]. Additionally, Vickstrom et al. [93] observed anxiolytic effects of endocannabinoid signaling in the MHB by depressing the synaptic GABA input in the ventral MHB from the medial septum and nucleus of the diagonal band. Such discrepancies may be derived from the different signaling pathways, animal models, and research methods used in these studies, as any of these factors can produce distinct behavioral manifestations. By contrast, we found that Y2 receptor activation mildly increased anxiety-like behaviors, similar to previous reports on the anxiogenic effects of NPY through Y2 receptors in the amygdala and lateral ventricles [94–96]. These results suggested that Y1

and Y2 receptors are expressed within different cell types and subtypes. The receptors may feature different neural circuits with potentially distinct functions. Furthermore, the responsiveness of NPY receptors can change under different conditions. Thorsell et al. [97] have demonstrated that overexpression of NPY in hippocampus of rats downregulated Y1 receptor binding but not Y2 receptor binding, suggesting subtype-specific functional changes of NPY receptors following NPY overexpression. In the present study, we surprisingly revealed that microinjection of NPY in VEH mice induced anxiety. This phenomenon could indicate that the Y1 receptor activity was down-regulated by NPY, and that Y2 receptor played a dominantly anxiogenic role in turn. After microinjecting NPY in GTN mice, the Y1 receptor mediated anxiolytic effects predominantly due to the upregulation of Y1 receptor expression by GTN (Fig. 6A). However, given that the precise mechanisms remain unclear, we will continue to pursue this matter in follow-up research.

Photophobia is one of the most common symptoms of migraine, and the underlying mechanism is uncertain. The anatomical structures of the potential neural circuits involved in the interaction between visual and pain pathways include the retina, olivary pretectal nucleus, superior salivatory nucleus, pterygopalatine ganglion, trigeminal afferents, trigeminal subnucleus caudalis, thalamus, hypothalamus, and cortex [98, 99]. Calcitonin gene-related peptide and pituitary cyclase-activating polypeptide are two important neuropeptides within photophobia circuits [100]. To date, no evidence has been found for the participation of MHb or NPY in photophobia, which is consistent with our findings that administration of NPY to MHb did not affect GTN-induced photophobia.

Conclusions

To the best of our knowledge, this is the first report of the analgesic and anxiolytic effects of NPY partly through Y1 receptors when microinjected into the MHb, using a GTN-induced migraine mouse model. These findings offer novel evidence for further development of therapeutic drugs. NPY targeting within the MHb might emerge as a new and effective migraine treatment. However, one limitation of the current study is the lack of evidence regarding Y1 receptor involvement using receptor antagonists or AAV-based RNA interference. Moreover, further studies will be needed to examine other potentially implicated brain regions, including the SPVO, NPC, PGRN, GU5, and SSp-n5, and determine how the NPY system contributes to migraine symptoms.

Abbreviations

EPM	Elevated plus maze
GTN	Glyceryl trinitrate
GU5	Gustatory areas layer 5
HMS	Hydrogel monomer solution
IPN	Interpeduncular nucleus
LP	Lateral posterior nucleus of the thalamus
MHb	Medial habenula
NPC	Nucleus of the posterior commissure
NPY	Neuropeptide Y
NTS	Nucleus of the solitary tract
PFA	Paraformaldehyde
PGRN	Paragigantocellular reticular nucleus
SPVC	Spinal nucleus of the trigeminal caudal part
SPVO	Spinal nucleus of the trigeminal oral part
SSp	Primary somatosensory area
SSp-n5	Primary somatosensory area nose layer 5
SSs	Supplemental somatosensory area
VEH	Vehicle
VISoR	Volumetric imaging with synchronized on-the-fly-scan and readout
VPM	Ventral posteromedial nucleus of the thalamus

Supplementary Information

The online version contains supplementary material available at <https://doi.org/10.1186/s10194-023-01596-z>.

Additional file 1: Figure S1. The total distance travelled during the EPM test at 2 h ($n = 8$ mice per group), 4 h ($n = 9$ mice per group), and 24 h ($n = 9$ mice per group) after VEH or GTN injection. (Related to Fig. 2) Significance was assessed by two-tailed unpaired Student's t-test. All data are presented as the mean \pm S.E.M. **Figure S2.** Effects of NPY or saline on the total distance travelled during the EPM test at 4 h after VEH or GTN injection. VEH + saline, $n = 11$ mice; GTN + saline, $n = 10$ mice; VEH + NPY, $n = 11$ mice; GTN + NPY, $n = 11$ mice. (Related to Fig. 5) Significance was assessed by two-way ANOVA. All data are presented as the mean \pm S.E.M. **Figure S3.** Effects of Y1 receptor agonist or Y2 receptor agonist on the total distance travelled during the EPM test at 4 h after VEH or GTN injection. GTN + saline, $n = 10$ mice; GTN + Y1 receptor agonist, $n = 11$ mice; GTN + Y2 receptor agonist, $n = 11$ mice. (Related to Fig. 7) Significance was assessed by one-way ANOVA. All data are presented as the mean \pm S.E.M. **Figure S4.** The representative images of histological sites of cannula placements in the MHb. Blue, 0.25% Evans Blue. Scale bars, 1000 μ m (A) and 200 μ m (B). The yellow contour delineates the borders of the MHb.

Additional file 2: Table S1. The quantitative number of NPY neurons in a maximum of 836 brain regions in VEH and GTN mice.

Acknowledgements

We thank technical support by the Hefei National Laboratory for Physical Sciences at the Microscale, and School of Life Sciences, University of Science and Technology of China. We appreciate Hao Wang, Guoqiang Bi, Wenjing Tang, Qi Jing, Lingxiao Guo, Wenguang Li and Dengfa Zhao for their technical assistance.

Authors' contributions

C.Y., S.Y., X.Z., and Z.D. carried out the study conceptualization and experimental design. C.Y., Z.G., S.M., X.H., and L.W. performed the behavioral tests. C.Y., Z.G., B.L., W.X., and T.W. performed imaging and cell counting. C.Y. wrote the manuscript. C.Y., X.Z., and S.Y. revised the manuscript. All authors contributed to the data analysis, and read and approved the final manuscript.

Funding

This work was supported by the National Natural Science Foundation of China (grants 82271242 and 82071226 to S.Y., 82171208 to Z.D., 81901134 to X.H.), the National Key Research and Development Program of China (grant 2022YFC2703600 to S.Y.), and the Logistics Support Research Project of China (grant 145BHQ090003000X12 to S.Y.).

Availability of data and materials

All data, reagents, resources, and protocols are available from the corresponding author upon reasonable requests.

Declarations**Ethics approval and consent to participate**

All data in this manuscript were collected from animals and all experimental procedures were approved by the Institutional Animal Care and Use Committee of the Chinese People's Liberation Army (PLA) General Hospital.

Consent for publication

Not applicable.

Competing interests

The authors declare that they have no competing interests.

Author details

¹School of Medicine, Nankai University, Tianjin 300071, China. ²Department of Neurology, the First Medical Center, Chinese PLA General Hospital, Fuxing Road 28, Haidian District, Beijing 100853, China. ³Medical School of Chinese PLA, Beijing 100853, China. ⁴Department of Medical Oncology, 980th Hospital of PLA Joint Logistical Support Force (Bethune International Peace Hospital), Shijiazhuang, Hebei 050082, China. ⁵Academy of Medical Engineering and Translational Medicine, Tianjin University, Tianjin 300072, China. ⁶Institute of Neuroscience, Zhejiang University School of Medicine, Hangzhou 310058, Zhejiang, China.

Received: 1 April 2023 Accepted: 15 May 2023

Published online: 25 May 2023

References

- Jensen R, Stovner LJ (2008) Epidemiology and comorbidity of headache. *Lancet Neurol* 7(4):354–361
- Oliveira R, Plácido M, Pereira L, Machado S, Parreira E, Gil-Gouveia R (2022) Headaches and the use of personal protective equipment in the general population during the COVID-19 pandemic. *Cephalalgia* 42(7):608–617
- Burstein R, Nosedá R, Borsook D (2015) Migraine: multiple processes, complex pathophysiology. *J Neurosci* 35(17):6619–6629
- Arnold M (2018) Headache classification committee of the international headache society (IHS) the international classification of headache disorders. *Cephalalgia* 38(1):1–211
- Bauer PR, Tolner EA, Keezer MR, Ferrari MD, Sander JW (2021) Headache in people with epilepsy. *Nat Rev Neurol* 17(9):529–544
- Breslau N, Lipton R, Stewart W, Schultz L, Welch K (2003) Comorbidity of migraine and depression: investigating potential etiology and prognosis. *Neurology* 60(8):1308–1312
- Tietjen G, Brandes J, Digre K, Baggaley S, Martin V, Recober A et al (2007) High prevalence of somatic symptoms and depression in women with disabling chronic headache. *Neurology* 68(2):134–140
- Kurth T, Chabriat H, Bousser M-G (2012) Migraine and stroke: a complex association with clinical implications. *Lancet Neurol* 11(1):92–100
- Schürks M, Winter A, Berger K, Kurth T (2014) Migraine and restless legs syndrome: a systematic review. *Cephalalgia* 34(10):777–794
- Vos T, Abajobir AA, Abate KH, Abbafati C, Abbas KM, Abd-Allah F et al (2017) Global, regional, and national incidence, prevalence, and years lived with disability for 328 diseases and injuries for 195 countries, 1990–2016: a systematic analysis for the Global Burden of Disease Study 2016. *Lancet* 390(10100):1211–1259
- Ferrari M, Goadsby P, Burstein R, Kurth T, Ayata C, Charles A et al (2022) Migraine. *Nat Rev Dis Prim* 8(1):2. <https://doi.org/10.1038/s41572-021-00328-4>
- Strother LC, Srikiatkachorn A, Suppronsinchai W (2018) Targeted orexin and hypothalamic neuropeptides for migraine. *Neurotherapeutics* 15(2):377–390
- Benarroch EE (2009) Neuropeptide Y: its multiple effects in the CNS and potential clinical significance. *Neurology* 72(11):1016–1020
- Chee MJ, Colmers WF (2008) Y eat? *Nutrition* 24(9):869–877
- Hökfelt T, Brumovsky P, Shi T, Pedrazzini T, Villar M (2007) NPY and pain as seen from the histochemical side. *Peptides* 28(2):365–372
- Heilig M (2004) The NPY system in stress, anxiety and depression. *Neuropeptides* 38(4):213–224
- Baraban S (2004) Neuropeptide Y and epilepsy: recent progress, prospects and controversies. *Neuropeptides* 38(4):261–265
- Gallai V, Sarchielli P, Trequattrini A, Paciaroni M, Usai F, Palumbo R (1994) Neuropeptide Y in juvenile migraine and tension-type headache. *Headache* 34(1):35–40
- Siva ZO, Uluduz D, Keskin FE, Erenler F, Balci H, Uygunoğlu U et al (2018) Determinants of glucose metabolism and the role of NPY in the progression of insulin resistance in chronic migraine. *Cephalalgia* 38(11):1773–1781
- Goadsby P, Edvinsson L, Ekman R (1990) Vasoactive peptide release in the extracerebral circulation of humans during migraine headache. *Ann Neurol* 28(2):183–187
- Vécsei L, Widerlöv E, Ekman R, Kovács K, Jelencsik I, Bozsik G et al (1992) Suboccipital cerebrospinal fluid and plasma concentrations of somatostatin, neuropeptide Y and beta-endorphin in patients with common migraine. *Neuropeptides* 22(2):111–116
- Valenzuela RF, Donoso MV, Mellado PA, Huidobro-Toro JP (2000) Migraine, but not subarachnoid hemorrhage, is associated with differentially increased NPY-like immunoreactivity in the CSF. *J Neurol Sci* 173(2):140–146
- Zhang L, Bijker MS, Herzog H (2011) The neuropeptide Y system: pathophysiological and therapeutic implications in obesity and cancer. *Pharmacol Ther* 131(1):91–113
- Naveilhan P, Hassani H, Lucas G, Blakeman KH, Hao J-X, Xu X-J et al (2001) Reduced antinociception and plasma extravasation in mice lacking a neuropeptide Y receptor. *Nature* 409(6819):513–517
- Chen L, Hu Y, Wang S, Cao K, Mai W, Sha W et al (2022) mTOR-neuropeptide Y signaling sensitizes nociceptors to drive neuropathic pain. *JCI insight*. <https://doi.org/10.1172/jci.insight.159247>
- Hwa JJ, Witten MB, Williams P, Ghibaudi L, Gao J, Salisbury BG et al (1999) Activation of the NPY Y5 receptor regulates both feeding and energy expenditure. *Am J Physiol Regul Integr Comp Physiol* 277(5):R1428–R1434
- Horio N, Liberles SD (2021) Hunger enhances food-odour attraction through a neuropeptide Y spotlight. *Nature* 592(7853):262–266
- Silva AP, Xapelli S, Grouzmann E, Cavadas C (2005) The putative neuroprotective role of neuropeptide Y in the central nervous system. *Current Drug Targets-CNS Neurol Disord* 4(4):331–347
- Di Clemente L, Coppola G, Magis D, Gérandy P, Fumal A, De Pasqua V et al (2009) Nitroglycerin sensitizes in healthy subjects CNS structures involved in migraine pathophysiology: evidence from a study of nociceptive blink reflexes and visual evoked potentials. *Pain* 144:156–161. <https://doi.org/10.1016/j.pain.2009.04.018>
- Demartini C, Greco R, Zanaboni AM, Sances G, De Icco R, Borsook D et al (2019) Nitroglycerin as a comparative experimental model of migraine pain: From animal to human and back. *Prog Neurobiol* 177:15–32
- van den Pol AN, Yao Y, Fu L-Y, Foo K, Huang H, Coppari R et al (2009) Neuromedin B and gastrin-releasing peptide excite arcuate nucleus neuropeptide Y neurons in a novel transgenic mouse expressing strong Renilla green fluorescent protein in NPY neurons. *J Neurosci* 29(14):4622–4639
- Percie du Sert N, Hurst V, Ahluwalia A, Alam S, Avey M, Baker M et al (2020) The ARRIVE guidelines 2.0: Updated guidelines for reporting animal research. *PLoS Biol* 18(7):e3000410. <https://doi.org/10.1371/journal.pbio.3000410>
- Harriott AM, Strother LC, Vila-Pueyo M, Holland PR (2019) Animal models of migraine and experimental techniques used to examine trigeminal sensory processing. *J Headache Pain* 20(1):1–15
- Pradhan AA, Smith ML, Zyuzin J, Charles A (2014) δ -Opioid receptor agonists inhibit migraine-related hyperalgesia, aversive state and cortical spreading depression in mice. *Br J Pharmacol* 171(9):2375–2384
- Zhang J, Czerpaniak K, Huang L, Liu X, Cloud M, Unsinger J et al (2020) Low-dose interleukin-2 reverses behavioral sensitization in multiple mouse models of headache disorders. *Pain* 161(6):1381–1398. <https://doi.org/10.1097/j.pain.0000000000001818>
- Paxinos G, Franklin KJB (2001) The mouse brain in stereotaxic coordinates, 2nd edn. Academic Press, San Diego

37. Pleil KE, Rinker JA, Lowery-Gionta EG, Mazzone CM, McCall NM, Kendra AM et al (2015) NPY signaling inhibits extended amygdala CRF neurons to suppress binge alcohol drinking. *Nat Neurosci* 18(4):545–552
38. Fendt M, Bürki H, Imobersteg S, Lingenhöhl K, McAllister KH, Orain D et al (2009) Fear-reducing effects of intra-amygdala neuropeptide Y infusion in animal models of conditioned fear: an NPY Y1 receptor independent effect. *Psychopharmacology* 206(2):291–301
39. Yang D-G, Gao Y-Y, Yin Z-Q, Wang X-R, Meng X-S, Zou T-F et al (2023) Roxadustat alleviates nitroglycerin-induced migraine in mice by regulating HIF-1 α /NF- κ B/inflammation pathway. *Acta Pharmacologica Sinica* 44(2):308–320
40. Markovics A, Kormos V, Gaszner B, Lashgarara A, Szoke E, Sandor K et al (2012) Pituitary adenylate cyclase-activating polypeptide plays a key role in nitroglycerol-induced trigeminovascular activation in mice. *Neurobiol Dis* 45(1):633–644
41. Elliott MB, Oshinsky ML, Amenta PS, Awe OO, Jallo JI (2012) Nociceptive neuropeptide increases and periorbital allodynia in a model of traumatic brain injury. *Headache* 52(6):966–84
42. Chaplan SR, Bach FW, Pogrel J, Chung J, Yaksh T (1994) Quantitative assessment of tactile allodynia in the rat paw. *J Neurosci Methods* 53(1):55–63
43. Christensen SL, Hansen RB, Storm MA, Olesen J, Hansen TF, Ossipov M et al (2020) Von Frey testing revisited: Provision of an online algorithm for improved accuracy of 50% thresholds. *Eur J Pain* 24(4):783–790
44. Wang H, Zhu Q, Ding L, Shen Y, Yang C-Y, Xu F et al (2019) Scalable volumetric imaging for ultrahigh-speed brain mapping at synaptic resolution. *Natl Sci Rev* 6(5):982–992
45. Wang Q, Ding S-L, Li Y, Royall J, Feng D, Lesnar P et al (2020) The Allen mouse brain common coordinate framework: a 3D reference atlas. *Cell* 181(4):936–53. e20
46. Bates E, Nikai T, Brennan K, Fu YH, Charles A, Basbaum A et al (2010) Sumatriptan alleviates nitroglycerin-induced mechanical and thermal allodynia in mice. *Cephalalgia* 30(2):170–178
47. Pradhan A, Smith M, McGuire B, Tarash I, Evans C, Charles A (2014) Characterization of a novel model of chronic migraine. *Pain* 155(2):269–274. <https://doi.org/10.1016/j.pain.2013.10.004>
48. Greco R, Meazza C, Mangione AS, Allena M, Bolla M, Amantea D et al (2011) Temporal profile of vascular changes induced by systemic nitroglycerin in the meningeal and cortical districts. *Cephalalgia* 31(2):190–198
49. Louter M, Pijpers J, Wardenaar K, Van Zwet E, Van Hemert A, Zitman F et al (2015) Symptom dimensions of affective disorders in migraine patients. *J Psychosom Res* 79(5):458–463
50. Zhang M, Liu Y, Zhao M, Tang W, Wang X, Dong Z et al (2017) Depression and anxiety behaviour in a rat model of chronic migraine. *J Headache Pain* 18(1):1–10
51. Kooshki R, Abbasnejad M, Esmaeili-Mahani S, Raof M, Sheibani V (2020) Activation orexin 1 receptors in the ventrolateral periaqueductal gray matter attenuate nitroglycerin-induced migraine attacks and calcitonin gene related peptide up-regulation in trigeminal nucleus caudalis of rats. *Neuropharmacology* 178:107981
52. Shelton L, Becerra L, Borsook D (2012) Unmasking the mysteries of the habenula in pain and analgesia. *Prog Neurobiol* 96(2):208–219
53. Intondi A, Dahlgren M, Eilers M, Taylor B (2008) Intrathecal neuropeptide Y reduces behavioral and molecular markers of inflammatory or neuropathic pain. *Pain* 137(2):352–365. <https://doi.org/10.1016/j.pain.2007.09.016>
54. Loh K, Herzog H, Shi Y-C (2015) Regulation of energy homeostasis by the NPY system. *Trends Endocrinol Metab* 26(3):125–135
55. Nelson TS, Taylor BK (2021) Targeting spinal neuropeptide Y1 receptor-expressing interneurons to alleviate chronic pain and itch. *Prog Neurobiol* 196:101894
56. Vázquez-León P, Ramírez-San Juan E, Marichal-Cancino BA, Campos-Rodríguez C, Chávez-Reyes J, Miranda-Páez A (2020) NPY-Y1 receptors in dorsal periaqueductal gray modulate anxiety, alcohol intake, and relapse in Wistar rats. *Pharmacol Biochem Behav* 199:173071
57. Oliveira M-M, Akerman S, Tavares I, Goadsby PJ (2016) Neuropeptide Y inhibits the trigeminovascular pathway through NPY Y1 receptor: implications for migraine. *Pain* 157(8):1666
58. Guo Y, Cheng Y, An J, Qi Y, Luo G (2021) Neuropeptide changes in an improved migraine model with repeat stimulations. *Transl Neurosci* 12(1):523–532
59. Hikosaka O (2010) The habenula: from stress evasion to value-based decision-making. *Nat Rev Neurosci* 11(7):503–513
60. Boulos L-J, Darcq E, Kieffer BL (2017) Translating the habenula—from rodents to humans. *Biol Psychiatr* 81(4):296–305
61. Darcq E, Befort K, Koebel P, Pannetier S, Mahoney MK, Gaveriaux-Ruff C et al (2012) RSK2 signaling in medial habenula contributes to acute morphine analgesia. *Neuropsychopharmacology* 37(5):1288–1296
62. Yamaguchi T, Danjo T, Pastan I, Hikida T, Nakanishi S (2013) Distinct roles of segregated transmission of the septo-habenular pathway in anxiety and fear. *Neuron* 78(3):537–544
63. Xu C, Sun Y, Cai X, You T, Zhao H, Li Y et al (2018) Medial habenula-interpeduncular nucleus circuit contributes to anhedonia-like behavior in a rat model of depression. *Front Behav Neurosci* 12:238
64. Zhang J, Tan L, Ren Y, Liang J, Lin R, Feng Q et al (2016) Presynaptic excitation via GABAB receptors in habenula cholinergic neurons regulates fear memory expression. *Cell* 166(3):716–728
65. Fowler C, Lu Q, Johnson P, Marks M, Kenny P (2011) Habenular α 5 nicotinic receptor subunit signalling controls nicotine intake. *Nature* 471(7340):597–601. <https://doi.org/10.1038/nature09797>
66. Wang J-Z, Lundeberg T, Yu L-C (2001) Anti-nociceptive effect of neuropeptide Y in periaqueductal grey in rats with inflammation. *Brain Res* 893(1–2):264–267
67. Alhadeff AL, Su Z, Hernandez E, Klima ML, Phillips SZ, Holland RA et al (2018) A neural circuit for the suppression of pain by a competing need state. *Cell* 173(1):140–52. e15
68. Solway B, Bose SC, Corder G, Donahue RR, Taylor BK (2011) Tonic inhibition of chronic pain by neuropeptide Y. *Proc Natl Acad Sci* 108(17):7224–7229
69. Shelton L, Pendse G, Maleki N, Moulton EA, Lebel A, Becerra L et al (2012) Mapping pain activation and connectivity of the human habenula. *J Neurophysiol* 107(10):2633–2648
70. Zhang C, Lai Y, Zhang Y, Xu X, Sun B, Li D (2021) Deep brain stimulation-induced transient effects in the habenula. *Front Psychiatry* 12:674962
71. Strotmann B, Kögler C, Bazin P-L, Weiss M, Villringer A, Turner R (2013) Mapping of the internal structure of human habenula with ex vivo MRI at 7T. *Front Hum Neurosci* 7:878
72. Strotmann B, Heidemann RM, Anwender A, Weiss M, Trampel R, Villringer A et al (2014) High-resolution MRI and diffusion-weighted imaging of the human habenula at 7 tesla. *J Magn Reson Imaging* 39(4):1018–1026
73. Antunes GF, Pinheiro Campos AC, de Assis DV, Gouveia FV, de Jesus Seno MD, Pagano RL et al (2022) Habenula activation patterns in a preclinical model of neuropathic pain accompanied by depressive-like behaviour. *PLoS One* 17(7):e0271295
74. Mészáros J, Gajewska S, Tarchalska-Kryńska B (1985) Habenulo-interpeduncular lesions: the effects on pain sensitivity, morphine analgesia and open-field behavior in rats. *Pol J Pharmacol Pharm* 37(4):469–477
75. Kitchen I, Slowe SJ, Matthes HW, Kieffer B (1997) Quantitative autoradiographic mapping of μ -, δ - and κ -opioid receptors in knockout mice lacking the μ -opioid receptor gene. *Brain Res* 778(1):73–88
76. Le Merrer J, Becker JA, Befort K, Kieffer BL (2009) Reward processing by the opioid system in the brain. *Physiol Rev* 89(4):1379–1412
77. Yang N, Anapindi KD, Rubakhin SS, Wei P, Yu Q, Li L et al (2018) Neuropeptidomics of the rat habenular nuclei. *J Proteome Res* 17(4):1463–1473
78. Hashikawa Y, Hashikawa K, Rossi MA, Basiri ML, Liu Y, Johnston NL et al (2020) Transcriptional and spatial resolution of cell types in the mammalian habenula. *Neuron*. 106(5):743–58. e5
79. Lecat S, Belemnaba L, Galzi J-L, Bucher B (2015) Neuropeptide Y receptor mediates activation of ERK1/2 via transactivation of the IGF receptor. *Cell Signal* 27(7):1297–1304
80. Lima LB, Bueno D, Leite F, Souza S, Gonçalves L, Furigo IC et al (2017) Afferent and efferent connections of the interpeduncular nucleus with special reference to circuits involving the habenula and raphe nuclei. *J Comp Neurol* 525(10):2411–2442
81. Noseda R, Burstein R (2013) Migraine pathophysiology: anatomy of the trigeminovascular pathway and associated neurological symptoms, cortical spreading depression, sensitization, and modulation of pain. *Pain* 154(Suppl 1):S44–53. <https://doi.org/10.1016/j.pain.2013.07.021>

82. Sandkühler J, Gruber-Schoffnegger D (2012) Hyperalgesia by synaptic long-term potentiation (LTP): an update. *Curr Opin Pharmacol* 12(1):18–27. <https://doi.org/10.1016/j.coph.2011.10.018>
83. Vázquez-León P, Mendoza-Ruiz LG, Ramírez-San Juan E, Chamorro-Cevallos GA, Miranda-Páez A (2017) Analgesic and anxiolytic effects of [Leu31, Pro34]-neuropeptide Y microinjected into the periaqueductal gray in rats. *Neuropeptides* 66:81–89
84. Trent NL, Menard JL (2011) Infusions of neuropeptide Y into the lateral septum reduce anxiety-related behaviors in the rat. *Pharmacol Biochem Behav* 99(4):580–590
85. Śmiałowska M, Wierońska JM, Domin H, Zięba B (2007) The effect of intrahippocampal injection of group II and III metabotropic glutamate receptor agonists on anxiety; the role of neuropeptide Y. *Neuropsychopharmacology* 32(6):1242–1250
86. Eaton K, Sallee FR, Sah R (2007) Relevance of neuropeptide Y (NPY) in psychiatry. *Curr Top Med Chem* 7(17):1645–1659
87. Menard J, Treit D (1996) Lateral and medial septal lesions reduce anxiety in the plus-maze and probe-burying tests. *Physiol Behav* 60(3):845–853
88. Murphy CA, DiCamillo AM, Haun F, Murray M (1996) Lesion of the habenular efferent pathway produces anxiety and locomotor hyperactivity in rats: a comparison of the effects of neonatal and adult lesions. *Behav Brain Res* 81(1–2):43–52
89. Klemm WR (2004) Habenular and interpeduncular nuclei: shared components in multiple-function networks. *Med Sci Monit* 10(11):RA261–RA73
90. Pang X, Liu L, Ngolab J, Zhao-Shea R, McIntosh JM, Gardner PD et al (2016) Habenula cholinergic neurons regulate anxiety during nicotine withdrawal via nicotinic acetylcholine receptors. *Neuropharmacology* 107:294–304
91. Molas S, DeGroot SR, Zhao-Shea R, Tapper AR (2017) Anxiety and nicotine dependence: emerging role of the habenulo-interpeduncular axis. *Trends Pharmacol Sci* 38(2):169–180
92. Kobayashi Y, Sano Y, Vannoni E, Goto H, Suzuki H, Oba A et al (2013) Genetic dissection of medial habenula–interpeduncular nucleus pathway function in mice. *Front Behav Neurosci* 7:17
93. Vickstrom CR, Liu X, Liu S, Hu M-M, Mu L, Hu Y et al (2021) Role of endocannabinoid signaling in a septohabenular pathway in the regulation of anxiety-and depressive-like behavior. *Mol Psychiatry* 26(7):3178–3191
94. Sajdyk TJ, Schober DA, Smiley DL, Gehlert DR (2002) Neuropeptide Y-Y2 receptors mediate anxiety in the amygdala. *Pharmacol Biochem Behav* 71(3):419–423
95. Morales-Medina JC, Dumont Y, Benoit C-E, Bastianetto S, Flores G, Fournier A et al (2012) Role of neuropeptide Y Y1 and Y2 receptors on behavioral despair in a rat model of depression with co-morbid anxiety. *Neuropharmacology* 62(1):200–208
96. Bacchi F, Mathé AA, Jiménez P, Stasi L, Arban R, Gerrard P et al (2006) Anxiolytic-like effect of the selective neuropeptide Y Y2 receptor antagonist BIIIE0246 in the elevated plus-maze. *Peptides* 27(12):3202–3207
97. Thorsell A, Michalkiewicz M, Dumont Y, Quirion R, Caberlotto L, Rimondini R et al (2000) Behavioral insensitivity to restraint stress, absent fear suppression of behavior and impaired spatial learning in transgenic rats with hippocampal neuropeptide Y overexpression. *Proc Natl Acad Sci* 97(23):12852–12857
98. Okamoto K, Tashiro A, Chang Z, Bereiter DA (2010) Bright light activates a trigeminal nociceptive pathway. *Pain* 149(2):235–242. <https://doi.org/10.1016/j.pain.2010.02.004>
99. Noseda R, Kainz V, Jakubowski M, Gooley JJ, Saper CB, Digre K et al (2010) A neural mechanism for exacerbation of headache by light. *Nat Neurosci* 13(2):239–245
100. Wang Y, Wang S, Qiu T, Xiao Z (2022) Photophobia in headache disorders: characteristics and potential mechanisms. *J Neurol* 269(8):4055–4067

Publisher's Note

Springer Nature remains neutral with regard to jurisdictional claims in published maps and institutional affiliations.

Ready to submit your research? Choose BMC and benefit from:

- fast, convenient online submission
- thorough peer review by experienced researchers in your field
- rapid publication on acceptance
- support for research data, including large and complex data types
- gold Open Access which fosters wider collaboration and increased citations
- maximum visibility for your research: over 100M website views per year

At BMC, research is always in progress.

Learn more biomedcentral.com/submissions

